

1 Evaluating the dendroclimatological potential of blue intensity on 2 multiple conifer species from **Tasmania and New Zealand**

3 Rob Wilson^{1,4}, Kathy Allen², Patrick Baker², Gretel Boswijk³, Brendan Buckley⁴, Edward Cook⁴,
4 Rosanne D'Arrigo⁴, Dan Druckenbrod⁵, Anthony Fowler³, Margaux Grandjean¹, Paul Krusic⁶, Jonathan
5 Palmer⁷

6 ¹ School of Earth & Environmental Sciences, University of St. Andrews, UK

7 ² School of Ecosystem and Forest Sciences, University of Melbourne, 500 Yarra Boulevard, Richmond 3121, Australia

8 ³ Tree-Ring Laboratory, School of Environment, The University of Auckland, Private Bag 92019, Auckland, New Zealand

9 ⁴ Lamont-Doherty Earth Observatory, Palisades, New York 10964, USA

10 ⁵ Department of Geological, Environmental, and Marine Sciences, Rider University, 2083 Lawrenceville Rd, Lawrenceville,
11 NJ, 08648, USA

12 ⁶ Department of Geography, University of Cambridge, Cambridge, UK

13 ⁷ School of Biological, Earth and Environmental Sciences, University of New South Wales, Sydney, NSW 2052, Australia

14 Correspondence to: Rob Wilson (rjsw@st-andrews.ac.uk)

15 **Abstract.** We evaluate a range of blue intensity (BI) tree-ring parameters in eight conifer species (12 sites) from Tasmania
16 and New Zealand for their dendroclimatic potential, and as surrogate wood anatomical proxies. Using a dataset of ca. 10-15
17 trees per site, we measured earlywood maximum blue intensity (EWB), latewood minimum blue intensity (LWB) and the
18 associated delta blue intensity (DB) parameter for dendrochronological analysis. No resin extraction was performed,
19 impacting low-frequency trends. Therefore, we focused only on the high-frequency signal by detrending all tree-ring and
20 climate data using a 20-year cubic smoothing spline. All BI parameters express low relative variance and weak signal
21 strength compared to ring-width. Correlation analysis and principal component regression experiments identified a weak and
22 variable climate response for most ring-width chronologies. However, for most sites, the EWB data, despite weak signal
23 strength, expressed strong coherence with summer temperatures. Significant correlations for LWB were also noted, but the
24 sign of the relationship for most species is opposite to that reported for all conifer species in the Northern Hemisphere. DB
25 results were mixed but performed better for the Tasmanian sites when combined through principal component regression
26 methods than for New Zealand. Using the full multi-species/parameter network, excellent summer temperature calibration
27 was identified for both Tasmania and New Zealand ranging from 52% to 78% explained variance for split periods (1901-
28 1950 / 1951-1995), with equally robust independent validation (Coefficient of Efficiency = 0.41 to 0.77). Comparison of the
29 Tasmanian BI reconstruction with a quantitative wood anatomical (QWA) reconstruction shows that these parameters record
30 essentially the same strong high-frequency summer temperature signal. Despite these excellent results, a substantial
31 challenge exists with the capture of potential secular scale climate trends. Although DB, band-pass and other signal
32 processing methods may help with this issue, substantially more experimentation is needed in conjunction with comparative
33 analysis with ring density and QWA measurements.

Formatted

Deleted: Australasia

Deleted: ⁵

Deleted: Sarah Blake³,

Deleted: ⁴

Deleted: ⁵

Deleted: ⁵

Deleted: ⁵

Deleted: ⁶

Deleted: ⁴

Deleted: ⁷

Deleted: ³

Deleted: School of Biological, Earth and Environmental Sciences,
University of New South Wales, Sydney, NSW 2052, Australia⁴

Deleted: ⁵

Deleted: ⁶

Deleted: ⁷

Deleted: reflectance

Deleted: reflectance

Deleted:

Deleted:

Deleted: calibrations

Deleted: well

Deleted: for the Tasmanian sites

Deleted: but explained minimal temperature variance in

Deleted:

Deleted: quantitative WA

61 1 Introduction

62 The range of variables that are now routinely measured from the rings of trees, including width, stable isotopes, multiple
63 wood anatomical properties and density, has increased substantially in recent years (McCarroll et al. 2002; McCarroll and
64 Loader, 2004; Drew et al. 2013; von Arx et al. 2016; Björklund et al., 2020). However, our knowledge of the climatic,
65 environmental, and physiological processes that modulate the year-to-year variability of these different tree-ring parameters
66 is still far from comprehensive.

67
68 Since the early seminal work of Fritts et al. (1965), a well-known rule of thumb for ring-width (RW) based
69 dendroclimatology is that trees sampled near their high elevation or latitude treelines will be predominantly temperature
70 limited, while at lower elevations or latitudes, moisture limitation becomes the primary driver of growth (Fritts 1976;
71 Kienast et al. 1987; Buckley et al. 1997; Wilson and Hopfmüller 2001; Briffa et al., 2002; Babst et al. 2013; St. George
72 2014). Such targeted sampling is strategically vital in “traditional” dendroclimatology and robust reconstructions can be
73 derived so long as tree-line sites are sampled where a single dominant climate parameter controls growth (Bradley 1999).
74 However, the climatic influence on RW can be complex and there are many published studies where the relationship
75 between RW and climate is shown to be temporally unstable and/or non-linear (Wilmking et al. 2020).

76
77 Ring density parameters, especially maximum latewood density (MXD), have been shown to provide substantially more
78 robust estimates of past summer temperature compared to RW (Briffa et al., 2002; Wilson and Luckman, 2003; Esper et al.,
79 2012; Büntgen et al., 2017; Ljungqvist et al., 2020). Density data may also retain a strong temperature signal at elevations
80 below the upper treeline, minimising the non-linear influence of a changing tree-line elevation through time (Kienast et al.
81 1987). The use of ring-density variables from lower elevation or latitude sites to reconstruct past hydroclimate is rare
82 (Camarero et al. 2014, 2017; Cleaveland 1986; Seftigen et al. 2020) and is clearly an area demanding further attention.

83
84 The reconstructive value of tree ring stable isotopes (carbon and oxygen) appears to be less constrained for sites where
85 climate does not limit growth and substantial potential exists from mid-latitude regions where traditional
86 dendroclimatological approaches are less reliable (McCarroll and Loader, 2004; Loader et al. 2008; Young et al. 2015;
87 Loader et al. 2020; Büntgen et al. 2021). However, within the mechanistic framework of stable isotopes, there is still much
88 to explore regarding the complex associations between fractionation and climate for different species and across different
89 ecotones.

90
91 The use of quantitative wood anatomical (QWA) parameters for dendroclimatology has gained traction in recent years due to
92 improvements in measurement methodologies allowing for the development of well-replicated chronologies for multiple
93 different anatomical variables (Drew et al. 2013; von Arx et al. 2016; Prendin et al., 2017; Björklund et al. 2020). The

Deleted: features

Deleted: or is unexpected but consistent between many sites (Cook and Pederson 2011).¶

Deleted: to climate limited locations

Deleted:

99 strength of relationships between climate parameters and wood anatomical properties such as latewood cell wall thickness,
100 tracheid radial diameter and microfibril angle is comparable to and can be stronger than maximum latewood density (Yasue
101 et al., 2000; Wang et al., 2002; Panyushkina et al., 2003; Fonti et al., 2013; Allen et al. 2018).

102
103 Despite the strong climate signal often noted in such non-RW tree-ring parameters, their procurement is expensive, often
104 requires specialised equipment and experience, and is time consuming. Consequently, there are substantially less published
105 data available for inspection and assessment. In recent years, blue intensity (BI) has been championed by many groups as a
106 cheaper surrogate for maximum latewood density (Björklund et al., 2014, 2015; Rydval et al., 2014; Wilson et al., 2014;
107 Kaczka and Wilson 2021). In its common usage, BI measures the intensity of the reflectance of blue light from the latewood
108 of scanned conifer samples so that a dense (dark) latewood would result in low intensity values. MXD and BI essentially
109 measure similar wood properties. Most studies that have directly compared MXD and latewood BI show no significant
110 difference in the climate response of the two parameters (Wilson et al., 2014; Björklund et al. 2019; Ljungqvist et al., 2020;
111 Reid and Wilson 2020). Though the acceptance of BI in dendrochronology was initially slow after the publication of the
112 original concept paper (McCarroll et al. 2002), over the past decade many BI-based studies have been published (Kaczka and
113 Wilson 2021). These studies have examined the use of BI as an ecological and climatological indicator in a variety of conifer
114 species from several locations around the Northern Hemisphere (Campbell et al., 2007, 2011; Helama et al., 2013; Rydval
115 et al., 2014, 2017, 2018; Björklund et al., 2014, 2015; Wilson et al., 2014, 2017a, 2017b, 2019; Babst et al., 2016; Dolgova,
116 2016; Arbella et al., 2018; Buras et al., 2018; Fuentes et al., 2018; Kaczka et al., 2018; Wiles et al., 2019; Harley et al.
117 2020; Heeter et al. 2020; Reid and Wilson 2020; Davi et al. 2021).

118
119 Only three studies that utilise BI data south of 30°N have been published. Buckley et al. (2018) explored the potential of
120 reflectance parameters from the tropical conifer Fujian cypress (*Fokienia hodginsii*) from central Vietnam and found a
121 significant positive relationship between earlywood maximum BI and December-April maximum temperature. Although a
122 spring/early summer temperature signal is extant in Northern Hemisphere conifer minimum density data from temperature
123 limited sites (Björklund et al. 2017), correlations are generally not as strong as the earlywood results detailed by Buckley et
124 al. (2018). In the Southern Hemisphere, Brookhouse and Graham (2016) measured latewood BI from *Errinundra plum-pine*
125 (*Podocarpus lawrencei*) samples taken from the Australian Alps and identified a strong inverse ($r = -0.79$) relationship with
126 August-April maximum temperatures, suggesting substantial potential for this species if long-lived specimens could be
127 found. Finally, Blake et al. (2020) recently explored the climate signal in BI parameters measured from Silver pine (*Manoao*
128 *colensoi*) samples growing on New Zealand's South Island and found strong significant relationships between both
129 earlywood and latewood BI parameters and summer temperatures. Although the sign (positive) of the earlywood BI
130 relationship with temperature agreed with results detailed in other studies (Björklund et al. 2017; Buckley et al. 2018), the
131 latewood relationship was inverse to that detailed for Northern Hemisphere conifers (Briffa et al. 2002) and observed by
132 Brookhouse and Graham (2016). This difference in latewood response begs the intriguing question as to whether some

Deleted: reflectance

Formatted: Superscript

Deleted: the

135 Southern Hemisphere conifers may have evolved differently from their Northern Hemisphere counterparts, resulting in a
 136 different anatomical and physiological response to climate.

137
 138 Here we expand upon the pilot studies of Brookhouse and Graham (2016) and Blake et al. (2020) and explore the climate
 139 signal of BI parameters from several key conifer species from Tasmania and New Zealand. To minimise nomenclature
 140 confusion, we refer to the different BI parameters as earlywood blue intensity (EWB) and latewood blue intensity (LWB).
 141 Based on ecophysiological theory (Buckley et al. 2018) we posit that EWB, derived from maximum intensity values of the
 142 whole-ring reflectance spectrum, essentially provides a surrogate for mean lumen size of the earlywood cells, while LWB,
 143 derived from minimum reflectance values, reflects the relative density (i.e. the proportion of cell wall to lumen area) of the
 144 darker latewood cell walls. We further suggest these reflectance measures are useful surrogate measures of mean tracheid
 145 diameter and cell wall thickness, which are proven to be excellent proxies of past climate (Allen et al. 2018; Björklund et al.
 146 2019) but are laborious and expensive to measure directly. As well as undertaking a dendroclimatic assessment of multiple
 147 BI parameters from different Australasian conifers, our analysis will also identify which species would be a good focus for
 148 further BI and QWA measurement in the future. Improving terrestrial-based estimates of past temperature in the land-limited
 149 Southern Hemisphere (Neukom et al. 2014) will only be achieved by enhancing the strength of the calibrated signal that until
 150 recently has been characterized solely by ring-width data which generally express a weak temperature signal.

151

Site Name	Site code	Common name	Species	Latitude (S)	Longitude	Elevation (m)	No of series	No of trees	full period	period ≥ 3 series
TASMANIA										
Race Spur	RCS	Celery Top pine	<i>Phyllocladus aspleniifolius</i>	41.29	145.44	500-550	16	14	1788-1995	1795-1995
L. Mackenzie	MCK	Pencil pine	<i>Athrotaxis cupressoides</i>	41.41	146.23	1116	15	15	1771-2007	1780-2007
Cradle Mountain	CM	Pencil pine	<i>Athrotaxis cupressoides</i>	41.40	145.57	1050	15	15	1787-2001	1789-2001
Mt Weld West / Trout Lake	MWWTRL	King Billy pine	<i>Athrotaxis selaginoides</i>	43.00	146.34	950	17	9	1781-1998	1785-1998
Mt Read - KBP	MRD	King Billy pine	<i>Athrotaxis selaginoides</i>	41.50	145.32	900	13	6	1770-2010	1778-2010
Mt Read - HP	MHP	Huon pine	<i>Lagarostrobos franklinii</i>	41.50	145.32	1000	22	16	781-2002	1238-2001
John Butters Power Station (King River)	BUT	Huon pine	<i>Lagarostrobos franklinii</i>	42.15	145.30	60	10	10	1773-2008	1798-2008
NEW ZEALAND										
Puketi	PKL	NZ Kauri	<i>Agathis australis</i>	35.15	173.45	180	13	10	1674-2001	1737-2001
Huapal	HUP	NZ Kauri	<i>Agathis australis</i>	36.48	174.3	100	17	13	1664-2007	1723-2006
Flagstaff	FLC	NZ Cedar	<i>Libocedrus bidwillii</i>	42.30	171.43	280	12	7	1774-2004	1776-2004
Ahaura	AHA	Silver pine	<i>Manoao colensoi</i>	42.23	171.48	244	12	12	1750-2012	1750-2012
Doughboy, Stewart Island	DPP	Pink pine	<i>Halocarpus biformis</i>	46.59	167.43	230	20	12	1767-2010	1777-2010

152
 153

154 **Table 1: Chronology information for the seven Tasmanian and five New Zealand sites used in the study (see Figure 1).**

155

156 2 Data and Methods

157 Four tree species from Tasmania and four from New Zealand were targeted for analysis (Figure 1, Table 1) representing
 158 conifer species that have not only been the focus of previous dendrochronological studies, but each has the potential to
 159 produce climate proxy records substantially greater than 1000 years in length. Until recently, RW data were used for most

Deleted: to

Deleted: earlywood and latewood BI

Deleted: reflectance

Deleted: in

Deleted: , temperature sensitive

Deleted: we

Deleted: also assess the potential for furthering the analysis of

Deleted: wood anatomical

Deleted: parameters in Australasian dendroclimatology

Deleted:

Deleted: low performing

Deleted: 5

Deleted: used in previous dendrochronological

Deleted: more than

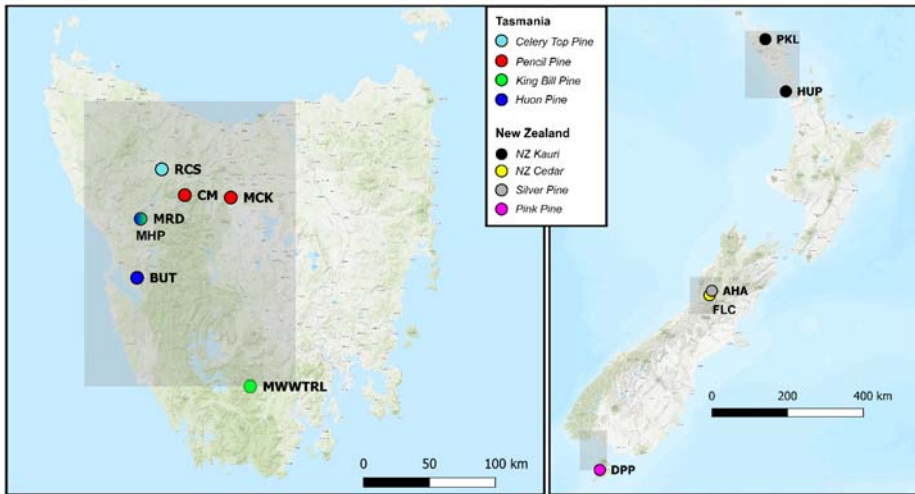
174 Australasian dendroclimatological studies, ~~with~~ calibration results never exceeding 40–45% explained variance. In Tasmania,
 175 the strongest calibration results for summer temperatures had been obtained using high elevation Huon pine (*Lagarostrobos*
 176 *franklinii* - Buckley et al. 1997; Cook et al. 2006) although some coherence was also found for Pencil pine (*Athrotaxis*
 177 *cupressoides*) and King Billy pine (*Athrotaxis selaginoides* - Allen et al. 2011; Allen et al. 2017). ~~The study sites (Table 1)~~
 178 ~~for Pencil pine (MCK and CM) and King Billy pine (MWWTRL and MRD) are located close to the upper timberline limit of~~
 179 ~~these species and growth is expected to be controlled mostly by summer temperatures. Likewise, the high elevation Huon~~
 180 ~~pine (MHP) site is also close to the upper treeline where summer temperature is the dominant response (Buckley et al. 1997).~~
 181 ~~However, BUT is located at the lower end of the Huon pine elevational range within a riparian environment so temperature~~
 182 ~~limitation is unlikely in a traditional sense. However, Drew et al (2013) identified strong summer temperature signals in~~
 183 ~~latewood QWA data for this site.~~ Celery Top (*Phyllocladus aspleniifolius*) RW data, however, express a complex non-linear
 184 relationship with climate ~~along its species' elevational range~~ and ~~have not been used for~~ dendroclimatic reconstruction
 185 (Allen et al. 2001). By contrast, summer temperature calibration experiments performed on measurement series of several
 186 wood anatomical properties ~~(e.g. tracheid radial diameter, cell wall thickness and microfibril angle), as well as RW and ring~~
 187 ~~density,~~ from these same species, have shown substantial improvement ~~over RW alone~~ (Allen et al. 2018), ~~although these~~
 188 ~~QWA data have been more useful for~~ hydroclimate reconstructions (Allen et al. 2015a/b). In New Zealand, RW-based
 189 summer temperature reconstructions have been developed from NZ Cedar (*Libocedrus bidwillii* - Palmer and Xiong 2004),
 190 Silver pine (*Manoao colensoi* - Cook et al. 2002, 2006) and Pink pine (*Halocarpus biformis* - D'Arrigo et al. 1996, Duncan
 191 et al. 2010) although ring density (Xiong et al. 1998 – Pink pine) and BI (Blake et al. 2020 – Silver pine) measured from ~~the~~
 192 ~~earlywood have produced stronger results. For this study, we specifically measured BI from samples used in previous,~~
 193 ~~mostly RW-based dendroclimatic, studies where summer temperature was found to be the dominant climate signal - at least~~
 194 ~~for NZ Cedar, Silver pine and Pink pine. The sites for these three New Zealand species are close to their southern~~
 195 ~~(latitudinal) limits (especially the Stewart Island Pink pine site) which is thought to compensate, to some degree, for their~~
 196 ~~modest elevational range (Table 1). Kauri (*Agathis australis*) is the longest-lived tree species in Australasia (Boswijk et al.~~
 197 ~~2014) but only a few sites of reasonably mature trees exist. Previous analyses have identified a complex mixed response to~~
 198 ~~both temperature and precipitation through the growing season (Buckley et al 2000, Fowler et al. 2000). However, it is~~
 199 ~~notable that Kauri RW data express a strong stable relationship with indices of the El Nino Southern Oscillation (Cook et al.~~
 200 ~~2006; Fowler et al. 2012).~~

Deleted:
Deleted: but
Deleted: ed
Deleted: (Allen et al. 2018).

Deleted: has

Deleted: s
Deleted: as well as the development of
Deleted:

Deleted: cells
Deleted: Kauri (*Agathis australis*) is the longest-lived tree species in Australasia (Boswijk et al. 2014) and is notable in that it expresses a strong stable relationship with indices of the El Nino Southern Oscillation (Cook et al. 2006; Fowler et al. 2012). For this study, we



215
216
217 **Figure 1:** Location map (basemap ESRI 2021) of the tree-ring sites used in this study (see Table 1). Also indicated (grey boxes) are
218 the regional domains of the gridded CRU TS 4.03 temperature and precipitation data (Harris et al., 2014) used for analyses.
219 Tasmania: 145-147°E / 41-43°S; New Zealand: North: 173-175°E / 35-37°S; Central: 171-172°E / 42-43°S; South: 167-168°E / 46-
220 47°S.

221
222
223 In this study, we utilised tree cores sampled over the past three decades that has been prepared for RW measurement.
224 Considering the focus of this study is to assess the potential of BI parameters for enhancing dendroclimatic reconstruction,
225 and the fact that the samples were already mounted, no resin extraction was performed except for the Silver pine AHA site
226 (see Blake et al. 2020 for details). As many of the species are resinous by nature, this immediately imposes a potential
227 problem for measuring BI data, because any inhomogeneous resin-related discolouration will impact intensity values
228 (Rydval et al., 2014; Björklund et al., 2014, 2015; Wilson et al. 2017b; Reid and Wilson 2020). Consequently, as the high-
229 frequency signal will only be minimally affected by discolouration (Wilson et al. 2017a), all analyses for this proof-of-
230 concept study will utilise only the high-pass fraction of the chronologies.

231
232 The mounted samples were re-sanded using fine grade (> 600 grit) sandpaper to remove decadal markings. Samples were
233 scanned at multiple institutions using different scanners and a range of resolutions from 1200 to 3200 DPI. RW and BI data
234 were generated using Coorecorder (Cybis 2016, <http://www.cybis.se/forfun/dendro/index.htm>) except for AHA

Deleted: o

Deleted: 167-168oE / 46-47o

Formatted: Superscript

Formatted: Superscript

Deleted: 171-172oE / 42-43oS.

Formatted: Superscript

Deleted: and

Deleted: reflectance

Deleted:

Deleted:

242 (WinDendro – see Blake et al. 2020). Regardless of image resolution, the CooRecorder BI generation “window” was set to
243 roughly equate to two-thirds width of the sample while the window depth encompassed either the latewood or earlywood for
244 each ring. The BI data were extracted following the method detailed in Buckley et al. (2018). For LWB, mean reflectance
245 values were taken from the lowest 15% of the darkest pixels, while for EWB the mean of the brightest 85% of the pixels was
246 used. Despite many of the samples being substantially older, most samples were measured only back into the 17th or 18th
247 centuries (with site MHP (Table 1) being an exception), providing enough data to ensure robust calibration and validation
248 over the instrumental period and to allow comparison with a temperature reconstruction from Tasmania based on QWA data
249 (Allen et al. 2018). Parameters generated for analysis were RW, EWB and LWB. As the study focuses only on the high-
250 frequency signal extant in the tree-ring data, the LWB data were not inverted as is the norm in Northern Hemisphere studies
251 using data generated in CooRecorder (Rydval et al. 2014).

252
253 Perhaps the greatest limitation for BI data parameters is that any colour changes that do not represent year-to-year changes in
254 wood anatomical features such as lumen size and cell wall thickness will impose a colour-related bias in the intensity
255 measurements. Examples of non-anatomically related colour changes are those associated with the heartwood/sapwood
256 transition, sections of highly resinous wood, or fungal staining. Björklund et al. (2014) proposed a statistical procedure that
257 could correct for such colour changes. This procedure subtracts the LWB reflectance value from the EWB data producing a
258 delta parameter (hereafter referred to as Delta BI - DB). Theoretically, DB should correct for common colour change biases
259 between heartwood and sapwood and even resinous zones within the wood. To date, DB has been utilised successfully in
260 only a few studies (Björklund et al., 2014, 2015; Wilson et al., 2017b; Fuentes et al. 2018; Blake et al. 2020; Reid and
261 Wilson 2020). As no resin extraction was performed (except site AHA, Table 1) and all the species used for this study
262 express a colour change from heartwood to sapwood, DB data will also be examined to explore its high-frequency
263 dendroclimatic potential.

264
265 For some of the studied species, the heartwood/sapwood transition colour change is very sharp and pronounced in
266 reflectance values (Figure A1), and inflexible detrending options could impose a systematic bias in the resultant detrended
267 indices. As an extreme example, the heartwood/sapwood transition of the EWB raw mean non-detrended chronology for the
268 CM Pencil pine site (Figure A2) cannot be tracked well with cubic smoothing splines (Cook and Peters 1981) of 200, 100 or
269 even 50 years respectively. This is not surprising given that the smoothing spline, operating as a symmetric digital filter, is
270 not well suited for dealing with abrupt changes in time series such as that observed in the CMewb chronology. In fact, the
271 bias of low (pre-transition) and high (post- transition) index values are only minimised when a flexible 20-year spline is used
272 because it better adapts to the observed discontinuity. However, this adaptability comes at the cost of losing potentially
273 valuable >20-year variability in the time series. This is clearly undesirable and better ways of modelling and removing such
274 discontinuities without the unwanted loss of lower-frequency variability are needed (see later discussion). Although less

Deleted: wood anatom

Deleted: y

Deleted: T

Deleted: light reflectance-based

Deleted: potential

280 flexible splines could be used for other species with a gradual or minimal colour change from heartwood to sapwood (Figure
281 A1), a consistent approach to detrending was deemed prudent and therefore a 20-year spline was used for all datasets.

Deleted: slower

282
283 The mean interseries correlation statistic (RBAR) is utilised to assess how many series are needed to attain an Expressed
284 Population Signal value of 0.85 (Wigley et al. 1984; Wilson and Elling 2004). Previous research has shown that the common
285 signal expressed by BI data can be rather weak (Wilson et al. 2014, 2017a/b, 2019; Kaczka et al. 2018; Wiles et al. 2019).
286 We explore this phenomenon further with this multi-parameter/species network by using the coefficient of variation to help
287 understand relative internal variance and covariance of the parameter chronologies.

Deleted: -

288
289 The climate signal expressed in the individual chronologies was initially explored using simple correlation analysis against
290 monthly gridded (see Figure 1 for locations) CRUTS 4.03 temperature and precipitation data (Harris et al. 2014) for the
291 periods 1902-1995, 1902-1950 and 1951-1995. Although the CRU TS data start in 1901, 1902 was the initial start year as
292 correlations were performed over 20 months including the previous growing season while 1995 reflects the final common
293 year for all tree-ring datasets (Table 1). The climate data were similarly detrended as the tree-ring data to ensure consistency.
294 Unsurprisingly, as most of the study sites are located in temperature limited upper tree-line locations, correlations with
295 monthly precipitation were weak, variable and temporally unstable for all species/parameter chronologies studies. The
296 results are presented in the Appendix but are not discussed further (see Table A4a-d).

Deleted: C

Deleted: and t

Deleted: Figure

297
298 Principal component analysis (PCA) was used on varying subsets of chronologies for each region (i.e. all chronologies of the
299 same parameter, or all parameters from a single species) to reduce the data to a few modes of common variance. Principal
300 components that had both an eigenvalue > 1.0 and correlated significantly (95% C.L.) with the target instrumental data were
301 entered into a stepwise multiple regression and calibrated against a range of seasonal temperatures. For New Zealand, the
302 three CRU TS 4.03 grid boxes (Figure 1) were averaged to create a countrywide mean series. This was justified as the three
303 inter-grid boxes mean correlation values between all tested seasons was 0.93 (STDEV = 0.01) suggesting there is a strong
304 common temperature signal between North Island and southern South Island. PCA was also utilised to ascertain the optimal
305 season for dendroclimatic calibration using the full chronology network for each country as well as exploring seasonal
306 differences between parameters and species. Analyses were performed over the common period of all tree-ring and climate
307 data (1901-1995) as well as early (1901-1950) and late (1951-1995) period calibration and verification. The Coefficient of
308 Efficiency (CE - Cook et al., 1994) was used to validate the regression-based climate estimates.

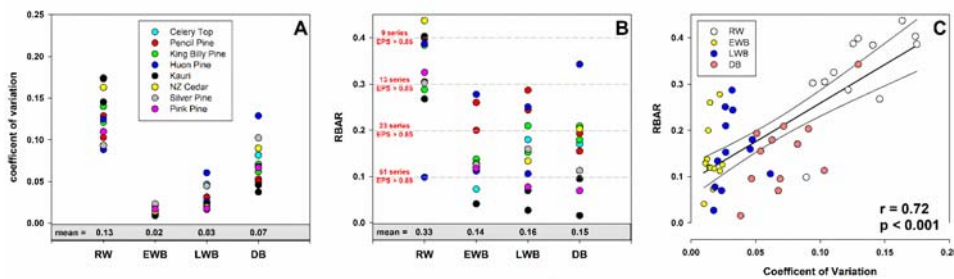
Deleted:

315 **3 Results and Discussion**

316 **3.1 Chronology variability and signal strength**

317 Wilson et al. (2014), using upper tree-line temperature-sensitive spruce samples from British Columbia, noted lower mean
 318 coefficient of variation (CV) values for LWB (0.05) compared to RW (0.28) and MXD (0.19). Common signal strength was
 319 strongest for the MXD data (RBAR = 0.42) while RW and LWB expressed similar but lower values, (0.30). For the
 320 Australasian detrended data, overall, RW data express higher relative variance (mean CV = 0.13) followed by DB (0.07),
 321 LWB (0.03) and EWB (0.02 – Figure 2a). The range in values for RW (0.09 – 0.17) and DB (0.04 - 0.13) are greater than
 322 LWB (0.02 - 0.06) although there is overlap in the range of DB and LWB. The EWB data express a significantly narrower
 323 range (0.01 - 0.02). RBAR values for the four different parameter groups generally return a stronger common signal for RW
 324 (mean = 0.33) compared with EWB (0.14), LWB (0.16), and DB (0.15 – Figure 2b). Therefore, following traditional
 325 methodologies to assess signal strength, more BI series are needed than RW to attain a robust chronology. On average across
 326 all sites, to attain an EPS value of at least 0.85 (Wigley et al. 1984), 14 series would be needed for RW, while 44, 47 and 58
 327 series would be needed for EWB, LWB and DB respectively. This weaker common signal of the BI parameters has been
 328 noted before (Wilson et al. 2014, 2017a/b, 2019; Kaczka et al. 2018; Wiles et al. 2019; Blake et al. 2020) and is also noted in
 329 QWA data from Tasmania (Allen et al. *in prep*). The common signal is particularly weak for Celery Top and Kauri (EWB)
 330 and Pink pine and Kauri (LWB and DB – see Table A1 for detailed values).

331



332

333

334 **Figure 2: A. Coefficient of variation (CV) of the 20-year spline detrended chronologies; B: mean inter-series correlation (RBAR) of**
 335 **the 20-year spline detrended series. Horizontal dashed lines denote the number of series needed for that particular RBAR value to**
 336 **attain an EPS of 0.85; C: Scatter plot of CV versus RBAR with linear regression.**

337

338

Deleted:

Deleted: were

Deleted: similar

Deleted: wood anatomica

Deleted: 1

344 A scatter plot of the CV and RBAR data (Figure 2c) suggests that the common signal expressed by these chronologies is
345 partly a function of the relative variance of the time-series ($r = 0.72$, $p < 0.001$). Although the range in RBAR values for the
346 EWB and LWB data suggests some uncertainty in this observation (see also Table A1), these results imply that the relatively
347 low variation of values around the mean for the BI parameters suggests that any anomalous colour staining on the wood that
348 does not reflect the true wood properties being measured could have a substantial impact on the chronology common signal.
349 However, it should be emphasised that a weak common signal and low EPS value does not necessarily result in a weak
350 climate signal (Buras 2017).

351 3.2 Climate response

352 The strength of correlations between the RW chronologies and mean monthly temperatures vary in sign and strength across
353 species. Over the full 1902-1995 period (Table 2), the Tasmanian MWWTRL (King Billy pine) and MHP (high elevation
354 Huon pine) sites express significant positive correlations with September-February and January-February respectively,
355 which are broadly time stable (Table A3a). RCS (Celery Top pine), MCK (Pencil pine) and MRD (King Billy pine) show
356 inverse correlations with late summer temperatures of the previous year. Of the New Zealand sites, PKL (Kauri) has negative
357 correlations for many months from winter through to the summer, while AHA (Silver pine) and DPP (Pink pine) correlate
358 positively with December-April and September- November.

359
360 Correlations between the EWB chronologies and mean temperatures are surprisingly consistent for most sites although
361 correlations for RCS (Celery Top pine) and BUT (low elevation Huon pine) are weak. Almost all site chronologies correlate
362 positively with the summer months for the current season – December through to March (Tasmania) and December-February
363 (New Zealand). The King Billy pine and Kauri sites express narrower (MMWTRL, MRD, PKL, and HUP) response
364 windows while DPP (Pink pine) is wider (Table 2). Although these relationships appear generally time stable, the Tasmanian
365 sites correlate more strongly with the narrower January-February season for 1902-1950 compared to the later post-1951
366 period (Table A3b). Significant correlations with winter and prior year temperatures are weaker and less consistent than for
367 current spring/summer. Overall, the consistent and strong correlations of EWB with summer temperatures are extremely
368 encouraging and show great promise for enhancing RW-based temperature reconstruction for both regions.

369
370 Significant relationships between LWB and summer and early Autumn temperatures are generally noted, although the results
371 are less consistent than those for EWB. Both RCS (Celery Top) and high elevation Huon pine (MHP) express negative
372 correlations that are in line with the positive MXD/temperature relationships noted in the Northern Hemisphere as the LWB
373 data are not inverted. Excluding MMWTRL (King Billy pine) and HUP (Kauri), which do not have any significant
374 correlations with temperature in the growing season, all the LWB chronologies express positive correlations with summer
375 and early autumn temperatures. This antithetic behaviour is not a new observation and has been noted by Drew et al. (2013),
376 O'Donnell et al. (2016), Blake et al. (2020) for latewood anatomical parameters, and LWB data, but these new results suggest

Deleted: the implication of these results is

Deleted: large

Deleted: ies

Deleted: Figure 3

Deleted: Figure

Deleted: Some

Deleted: or wider

Deleted: (

Deleted: - Figure 3

Deleted:

Deleted: Figure

Deleted: results

Deleted: (Celery Top)

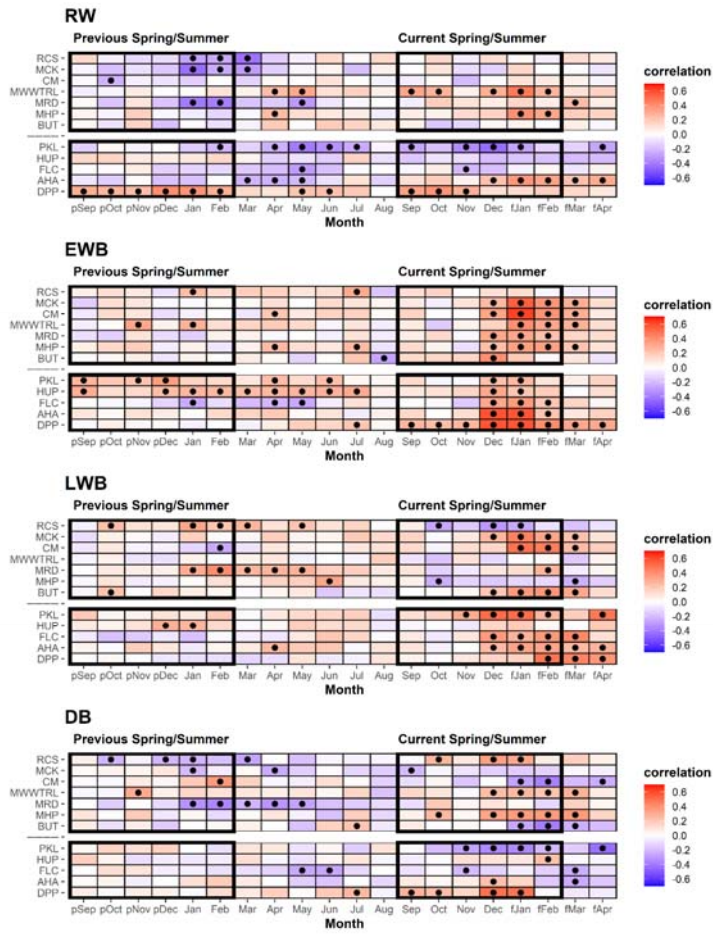
Deleted: that

Deleted: other species

Deleted: latewood wood anatomical parameters

393 that this physiological phenomenon is not based on a chance occurrence of a single species and is consistent between several
 394 Australasian conifer tree species (Pencil pine, Huon pine (low elevation), Kauri, NZ Cedar, Silver pine and Pink pine). Blake
 395 et al. (2020) explained the inverse LWB relationship as a reduction in the duration of secondary cell wall thickening in
 396 warmer years. Such “emergent” surprising results (Cook and Pederson 2011) clearly need further research and testing.
 397

Deleted: a number of



398

400 **Table 2:** Correlation response function analysis results for the different TR parameter chronologies with CRU TS temperatures.
401 Analysis undertaken over the 1902-1995 period (see supplementary figure S3 for correlations for split periods 1902-1950, 1951-
402 1995). **The upper block is for the Tasmanian sites, while the lower block is New Zealand. See Table 1 for site code names and**
403 **species. Black dots denoted correlations significant at the 95% C.L.**

404

405

406 The DB chronologies express a range of responses to temperature that are all generally weaker than for EWB and LWB
407 (Table 2). Significant positive correlations with summer temperatures are found for RCS (Celery Top), MMWTRL (King
408 Billy pine), MHP (Huon pine), and DPP (Pink pine). HUP (Kauri) and AHA (Silver pine) also express some weak positive
409 summer temperature coherence. Negative correlations are noted for CM (Pencil pine), BUT (low elevation Huon pine), PKL
410 (Kauri) and FLC (NZ Cedar). However, many of these correlations are not temporally stable when compared over the 1902-
411 1950 and 1951-1995 periods (Table A3d). Current theory suggests that DB should perform well when EWB and LWB
412 parameters are weakly correlated and express different earlier and later seasonal climate responses (Björklund et al., 2014).
413 However, the results herein indicate that this simple hypothesis does not consistently apply in this multi-species study. For
414 example, the EWB and LWB data for the Pink pine DPP site express different early (Sep-April) and late (Feb-Apr) seasonal
415 responses with temperatures (Table 2), but still show a reasonably high inter-parameter correlation (0.60, Table A2) although
416 this is partly expected as the response windows overlap. However, the DB data still expresses a significant and strong
417 response with summer temperatures, although marginally weaker than the EWB response. On the other hand, DB for the
418 Pencil pine sites (MCK and CM) behaves more like conifers in the Northern Hemisphere (Björklund et al., 2014; Wilson et
419 al. 2017b), with significant correlations noted for both EWB and LWB with summer temperatures, but, likely due to the high
420 inter-parameter correlation (0.57 and 0.68), the DB data express weak, or even inverse correlations with summer
421 temperatures. Overall, the DB results are mixed and disappointing. This parameter theoretically could minimise the colour
422 bias of the darker to lighter colour heartwood/sapwood transition (Figure A1) but, for the data used herein, as the high-
423 frequency signal often portrays a mixed or weak signal with temperature, it suggests that the DB parameter might not be a
424 valid approach to address the heartwood/sapwood transition bias. These results suggest that alternative approaches to using
425 DB may need to be explored to minimise the impact of the heartwood/sapwood change noted in most of the species used in
426 this study.

427 3.3 Parameter and species-specific principal component calibration tests

428 The previous section detailed that temperature is the predominant climate signal expressed across the Tasmanian and New
429 Zealand RW and BI data studied herein (Figures 3, A3a-d). Only weak coherence with precipitation was found (Table A4a-
430 d). To further explore the climate response, principal component regression calibration (1901-1995) experiments with
431 seasonal temperature were performed to ascertain which combination of BI parameters and species express the strongest
432 climate signal and therefore should be the focus for future research – including refined BI measurement and/or QWA
433 measurement.

Deleted: Figure

Deleted: 3

Deleted: Figure 3

Deleted: Figure

Deleted: Figure 3

Deleted: this appears not to be the case

Deleted: species and parameters in these chronologies from

Deleted: Figure

Deleted: wood anatomical

443

444 For Tasmania, the PCA identifies three (RW), two (EWB), two (LWB) and two (DB) principal components respectively.

445 Each BI parameter PC regression explains > 40% of the temperature variance while RW is substantially weaker at 21%

446 (Figure 3a). Both EWB and LWB explain 43% of the December-February and January-March variance respectively - these

447 seasons being biologically logical with respect to the earlier seasonal start for EWB and later end for LWB. Despite the site-

448 specific DB data correlating with temperature more weakly than EWB and LWB (Table 2), their multivariate combination

449 calibrates better (48%) with January-March temperatures. Although this is an encouraging result as DB may theoretically

450 correct for colour related biases, the mix of positive and negative zero-order correlations with temperature (Table 2) suggest

451 that some caution will be needed if such data are used to capture more secular scale information.

452

Deleted: 3, 2, 2 and 2 significant

Deleted: for RW, EWB, LWB and DB

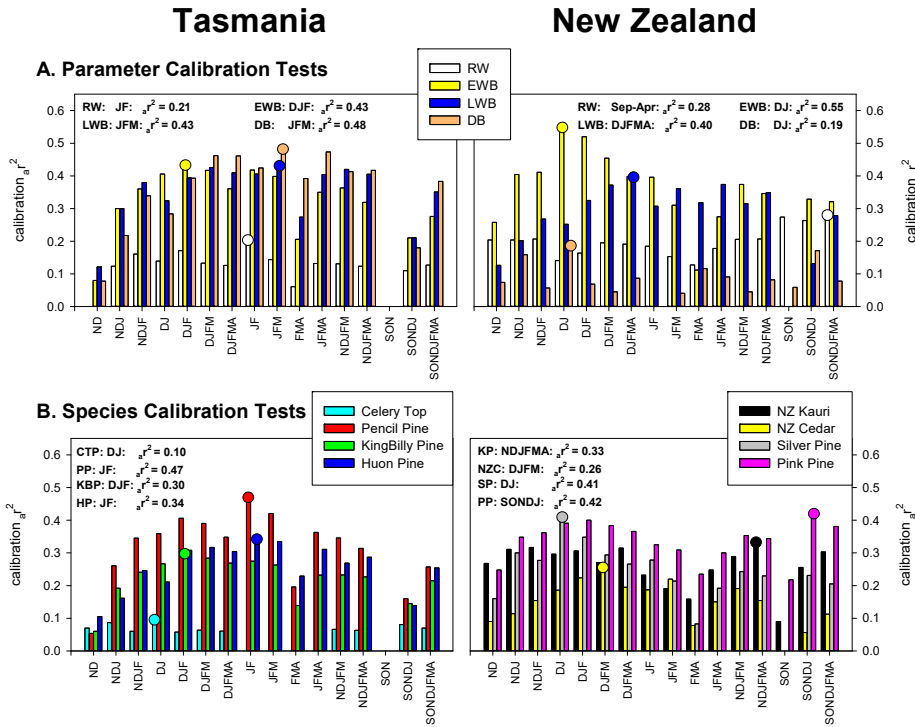
Deleted: poorer

Deleted: 4

Deleted: Figure 3

Deleted:

Deleted: Figure 3



453

461 **Figure 3: PC regression calibration (1901-1995) experiments for parameters (all species) (A) and species (all variables) (B). A**
462 **range of temperature seasonal targets are used with the strongest seasonal calibrations highlighted with circles.**

463

464 For New Zealand, PCA identifies 3, 2, 2 and 3 significant principal components for RW, EWB, LWB and DB respectively.
465 EWB calibrates very strongly (55%) with December-January temperatures while LWB explains 40% of the broader
466 December-April season (Figure 3a). Alone, RW explains 28% of the temperature variance but for a broad September-April
467 season which reflects the variable site-specific responses of PKL, AHA and DPP (Table 2). The DB data calibrate poorly
468 explaining only 19% of the December-January temperature variance.

469

470 Of all the species tested, Tasmanian Pencil pine returns the strongest calibration (47%) with January-February temperatures
471 (Figure 3b) although New Zealand Silver pine and Pink pine also calibrate reasonably with 41% (December-January) and
472 42% (September-January). It should be noted that two Pencil pine sites were used (Table 1) compared to only one each for
473 Silver pine and Pink pine which likely will influence these results. King Billy pine, Huon pine and Kauri explain 30%
474 (December-February), 34% (January-February) and 33% (November-April) respectively of the temperature variance with
475 New Zealand cedar still showing some reasonable coherence (26%) for December-March. Celery Top is the weakest species
476 explaining only 10% of the December-January temperature variance.

477 3.4 Region-wide calibration and validation

478 A multi-site, multi-species approach to dendroclimatology can improve overall calibration even if some of the sampled sites
479 and species are not located close to climate limited treeline ecotones (Alexander et al. 2019). Herein we have an opportunity
480 to pool all the data for each country to create combined multi-species and multi-parameter regional reconstructions. As the
481 optimal season for calibration varies as a function of species and parameter (Figure 3), initial PC regression experiments
482 using all chronologies from each of the two regions, were performed. For each of these models, all PCs with an eigenvalue
483 > 1.0 were entered into the regression model. January-February (JF) temperature was identified as the overall optimal season
484 for Tasmania while December-January (DJ) provided the strongest calibration for New Zealand. Forcing all variables into
485 the PC regression model also provides an opportunity to identify the importance of each species parameter towards the
486 development of regional reconstructions. The beta weights (Cook et al. 1994) from the regression modelling (Table 3)
487 clearly show the strong influence of the EWB parameters in the multiple regression model, especially from Pencil pine
488 (MCK and CM) and Silver pine (AHA) although strong beta weights are also noted for King Billy pine (MDR), Huon pine
489 (MHP) and Pink pine (DPP). Other parameters that provide useful information in the modelling are RW (King Billy pine
490 (MWWTRL) and Huon pine (MHP)), LWB (Pencil pine (MCK, CM), Huon pine (BUT) and Kauri (PKL)) and DB (Huon
491 pine (MHP) and Pink pine DPP). These results are consistent with the correlation response function analysis (Table 2), but
492 it must be emphasised that the results shown in Table 3 are related to specific seasons (JF for Tasmania and DJ for New
493 Zealand) and may not reflect the optimal season for individual species or parameters (Figure 3).

Deleted: 4

Deleted: both parameters

Deleted: 4

Deleted: Figure 3

Deleted: 4

Deleted: Of the species models (Figure 4b),

Deleted:

Deleted: a

Deleted: 4

Deleted: was

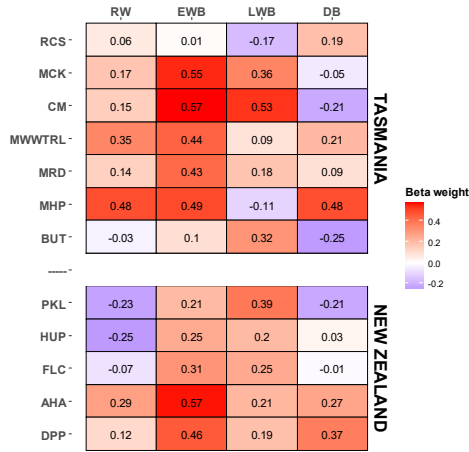
Deleted: 2

Deleted: Figure 3

Deleted: 2

Deleted: 4

508



509

510

511 Table 3: PC regression calibration (1901-1995) beta weights using all parameter and species data. The Tasmanian modelling was
 512 performed against January-February temperatures while New Zealand was with December-January.

513

514

515 For the final countrywide calibration and validation experiments, three PC regression approaches were used, each reflecting
 516 more stringent screening procedures; (1) as already detailed above - all data entered into PCA and PCs with an eigenvalue >
 517 1.0 that correlated significantly (95%) with the instrumental target were entered as possible candidates into a stepwise
 518 multiple regression; (2) same as (1) but chronologies were initially screened for significant correlation with the full period
 519 instrumental target before PCA; (3) similar to previous variants, but significant consistent correlations between the
 520 chronologies and the instrumental target for both the 1901-1950 and 1951-1995 periods were required.

521

522 For Tasmania, the initial 28 parameter chronologies were reduced to 17 and 10 respectively via the two more stringent
 523 screening procedures while the 20 initial chronologies from New Zealand were reduced to 13 and 7 respectively (Figure 4).
 524 Full period (1901-1995) calibration is excellent for all versions with the Tasmanian variants 1 and 2 expressing 63-64% of
 525 the JF temperature variance, reducing to 55% for variant 3. The New Zealand data return similarly good results with 61-64%
 526 of the DJ temperature variance being explained by all variants. Split period calibration and validation are equally good for all
 527 variants with the Tasmanian variants explaining 52-65% of the variance for all early/late period calibration while CE ranges

Deleted: 2
 Deleted:

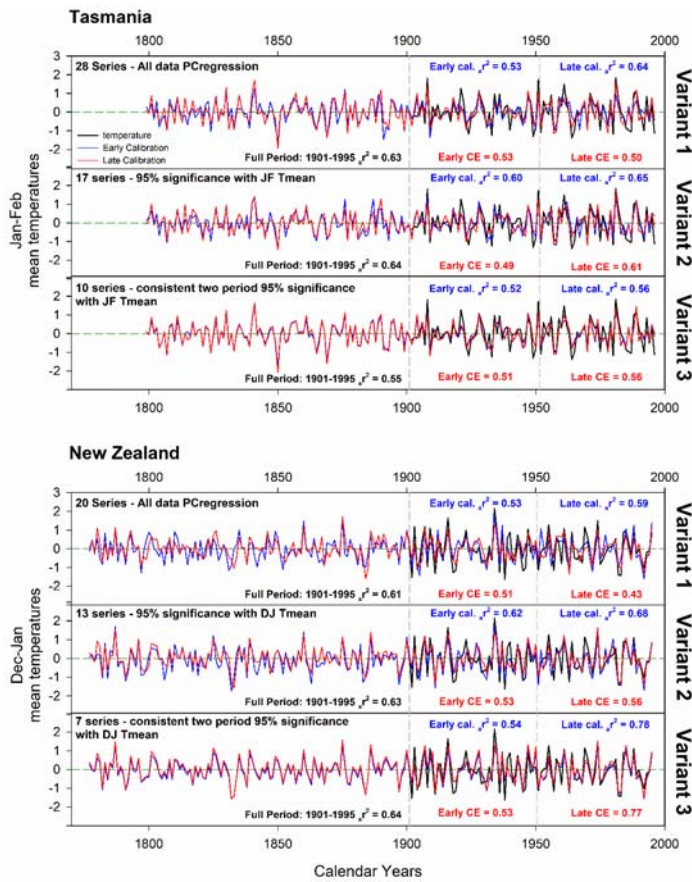
Deleted: 5

Deleted: is

532 from 0.49-0.61. Similar results are obtained for New Zealand with calibration adjusted r^2 (r^2) and CE values ranging from
 533 0.53-0.78 and 0.43-0.77 respectively. For both countries, calibration and validation are marginally stronger for the later
 534 1951-1995 period which might suggest some degree of uncertainty in the instrumental period in the early part of the 20th
 535 century.

536

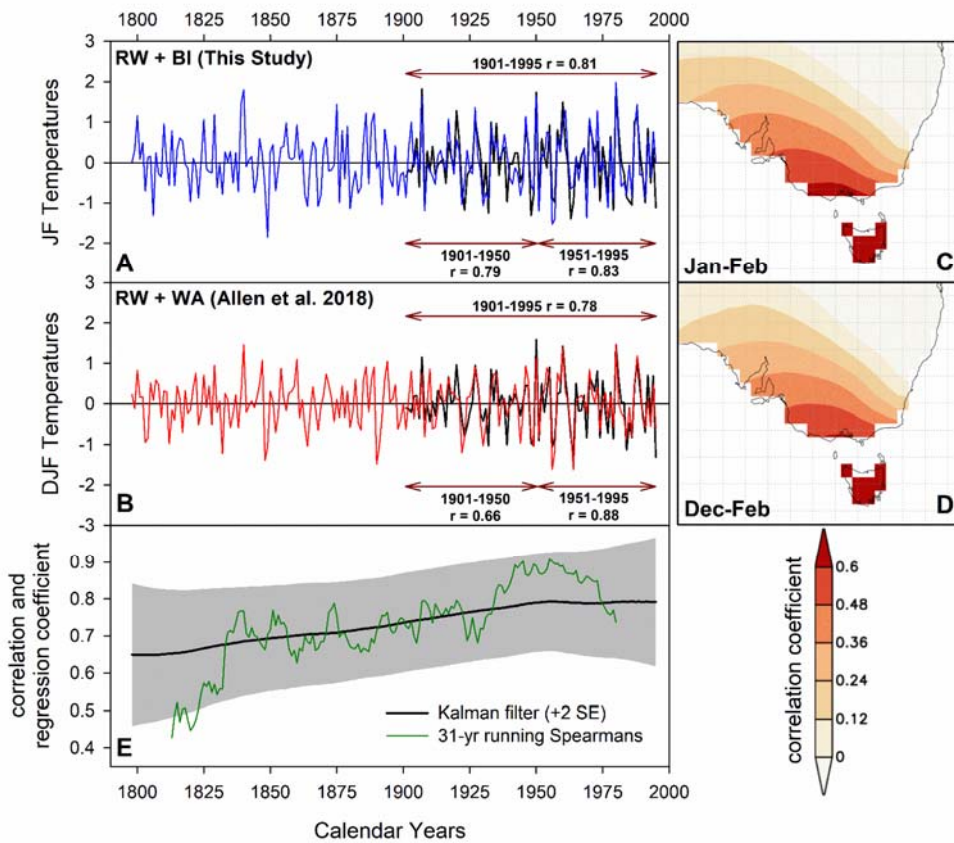
- Deleted: a
- Formatted: Superscript
- Formatted: Subscript
- Formatted: Superscript
- Deleted: was



537

538

541 Figure 4: Principal component regression results using all data (Variant 1), full period (1901-1995) screened data (Variant 2), and
 542 two-period screening (Variant 3). Split period calibration and validation were performed over 1901-1950 and 1951-1995.



543

544

545 Figure 5: A: Variant 2 (full period screened) Tasmanian JF temperature RW+BI parameter-based reconstruction with CRU TS
 546 temperature data. Pearson's correlation is shown for 1901-1995, 1901-1950 and 1951-1995 period; B: As A, but for Allen et al.
 547 (2018) RW+WA based Tasmanian DJF temperature reconstruction. These data have also been high-pass filtered using a 20-year
 548 cubic smoothing spline; C + D: Spatial correlations (1841-1995) between each reconstruction and similarly detrended Berkeley
 549 gridded data for the Jan-Feb and Dec-Feb seasons respectively; E: Running 31-year Spearman's rank correlation and Kalman
 550 filter analysis (Visser and Molenaar 1988).

Deleted: 5

Deleted:

Deleted: ¶

¶

Deleted: 6

Deleted:

Deleted: linearly

558

559 Overall, the temperature reconstruction experiments for both Tasmania and New Zealand (Figure 4) return excellent results
560 with overall calibration r^2 values well above 0.60. Although no QWA data exist yet for New Zealand, Allen et al. (2018)
561 recently produced a range of PC regression-based Tasmanian summer temperature reconstructions from a network of 58
562 chronologies using RW and QWA (mean tracheid radial diameter, mean cell wall thickness, mean density and microfibril
563 angle). These variables were measured using the SilviScan system (Evans, 1994) from the same four Tasmanian tree species
564 used herein using samples from the same region, but from more sites. Strong calibration results explaining 50-60% of the
565 temperature variance and robust validation were also noted in their analyses. We compare our full period screened
566 temperature reconstruction (Variant 2, Figure 4 – representing the most used data screening approach in dendroclimatology)
567 with a high-pass filtered (20-year spline) version of Allen et al.'s (2018) “Berkeley all-data” reconstruction variant (Figure
568 5). Both reconstructions correlate similarly with the CRU TS temperature data (1901-1995: RW/BI $r = 0.81$ (JF) and
569 RW/WA $r = 0.78$ (DJF) – Figure 5a/b) although the BI-based reconstruction expresses a slightly more stable response with
570 temperatures over the 1901-1950 and 1951-1995 periods ($r = 0.79$ and 0.83 vs 0.66 vs 0.88). However, as the BI-based
571 reconstruction was calibrated against these CRU TS data, this slight difference may simply reflect the optimised PC
572 regression fit to one instrumental dataset over another. Equivalent split period correlations using the Berkeley temperature
573 data (Rohde et al. 2013), as used by Allen et al. (2018), are $0.82/0.86$ (RW/BI) and $0.77-0.90$ (RW/WA).

574

575 Correlation with the Berkeley data over the 1841-1900 period, shows that coherence is weaker but similar between Allen et
576 al.'s (2018) and this study (0.54 and 0.66). The spatial representation of the reconstructed temperature signal in both datasets
577 is almost identical when using linearly detrended Berkeley gridded temperature data (Rohde et al. 2013) even when
578 including data back to 1841 (Figure 5c/d). Both reconstructions are strongly correlated with each other (Pearson's $r = 0.75$,
579 1798-1995) although this coherence weakens back in time as evidenced by both a running 31-year Spearman's rank
580 correlation and Kalman filter (Visser and Molenaar 1988), showing a peak coherence in the 20th century that decreases back
581 towards the early part of the 19th century (Figure 5e). This likely represents the decrease in sample replication through time
582 in some BI-based datasets (MWWTSL and BUT) used in this study (Figure A1). Overall, the BI data, at least for Tasmania,
583 basically express the same high-frequency signal as the WA data used in Allen et al. (2018) and the results herein suggest
584 that BI parameters could provide excellent proxies of past growing season temperatures. However, for their potential to be
585 truly realised, the heartwood/sapwood colour change and other discolouration issues need to be overcome.

586 4 Conclusions and future research directions

587 In this study, we measured a range of blue intensity parameters from eight conifer species from Tasmania and New Zealand
588 to ascertain whether the use of EWB, LWB and/or DB can improve upon previous RW-only based dendroclimatic
589 reconstructions that explain about 40-45% of the temperature variance. No attempt to remove resins was made for this proof-

Deleted: 5

Formatted: Subscript

Deleted: in excess of

Deleted: wood anatomical

Deleted: s

Formatted: Superscript

Deleted:

Deleted: ,

Deleted: 5

Deleted: 6

Deleted: 6

Deleted:

Deleted:

Deleted: 6

Deleted: 6

Deleted:

Deleted:

Deleted: bias

Deleted: s

607 of-concept study. Therefore, due to the impact on intensity-based parameters of resins and heartwood/sapwood colour
608 changes on the wood, we detrended the chronologies and climate data using a very flexible spline (20-years) to focus only on
609 the high-frequency signal. Metrics denoting signal strength (RBAR and EPS) indicated a very weak common signal in the BI
610 parameters (mean RBAR range 0.14 – 0.16, Figure 2b) compared to the RW data (mean RBAR = 0.33) which appeared to be
611 partly related to the relative variance in these datasets. The EWB data in particular exhibit very low variability which may
612 mean that any colour variation in the wood that does not reflect true year-to-year wood anatomical variance may have a large
613 impact on such data, thus weakening the common signal.

614
615 Despite the weak common signal expressed by the BI parameters, the climate signal extant in these data is very strong,
616 especially EWB. When all parameters are combined using PC regression, depending on the period used, 52-78% of the
617 summer temperature variance can be explained (Figure 4). This is generally greater than the norm for Northern Hemisphere
618 based MXD/BI-related temperature reconstructions (Wilson et al. 2016), although admittedly, the results in this study are
619 focused only on the high-frequency fraction of the data. These strong calibration results are driven mainly by EWB data
620 from Pencil pine, high elevation Huon pine and King Billy pine (Tasmania) and Silver pine, Pink pine and cedar (New
621 Zealand) although useful information was also identified in LWB (Pencil pine, low elevation Huon pine, Kauri and cedar),
622 DB (high elevation Huon pine and Pink pine) and RW (high elevation Huon pine – Table 3). However, the relationship of
623 LWB for most species with summer temperatures is opposite to that observed in the Northern Hemisphere and further study
624 is needed to assess the physiological processes leading to this inverse relationship in these particular Southern Hemisphere
625 conifers.

626
627 The similarity of the Tasmanian multi-TR-proxy reconstruction with a reconstruction heavily dependent on QWA data
628 (Allen et al. (2018) - Figure 5) clearly highlights that the BI and WA data express similar wood properties. This is a highly
629 encouraging result for the utilisation of BI as it is quicker and cheaper to produce than QWA data. However, the “elephant in
630 the room” is whether robust low-frequency information can be extracted from BI-based parameters or is it an analytical
631 methodology that ultimately will be relevant only for decadal and higher frequencies. It is unlikely that the
632 heartwood/sapwood colour change (both sharp and gradual – Figure A1), expressed by most of the tree species used in this
633 study, can be fully removed by resin extraction alone. Some success at overcoming heartwood/sapwood colour bias using
634 DB has been shown for some Northern Hemisphere conifer species (Björklund et al., 2014, 2015; Wilson et al., 2017b;
635 Fuentes et al. 2018; Reid and Wilson 2020), but the DB results detailed herein (Table 3, Figures 2- 4) suggest that DB may
636 not always provide a robust solution to the issue.

637
638 Other statistical approaches have been used to overcome the colour bias using either contrast adjustments (Björklund et al.,
639 2015; Fuentes et al., 2018) or band-pass approaches where the low-frequency signal is derived from the RW data and the
640 high frequency is driven by the BI data (Rydval et al., 2017) but further experimentation is needed. We hypothesise that

Deleted: reflectance

Deleted:

Deleted: 5

Deleted:

Deleted: s

Deleted:

Deleted: 2

Deleted: in sign

Deleted: wood anatomical

Deleted: 6

Deleted:

Deleted:

Deleted: 2

Deleted:

655 relatively sharp changes in colour intensity measures related to the heartwood/sapwood transition can be viewed
656 conceptually in a similar way to how endogenous disturbances affect ring-width parameters over time (Cook 1987). Similar
657 to the progress in developing growth release detection methods to reconstruct canopy disturbance histories of forests
658 (Altman 2020, Trotsiuk et al. 2018), radial growth averaging (Lorimer and Frelich 1989) or time series methods
659 (Druckenbrod et al., 2013; Rydval et al. 2016) could be used to identify and remove the colour bias signature resulting from
660 the change in physiology from heartwood to sapwood. However, to facilitate such signal processing methods, more studies
661 are needed to directly compare both MXD and QWA data with BI parameters to understand the secular trend biases in these
662 light intensity parameters. At the very least, the results detailed herein, based on a limited number of sites per species, show
663 that BI parameters can be used to identify those species that should be targeted for more costly and time-consuming
664 analytical methods such as QWA measurement.

Deleted: data

Deleted: reflectance

Deleted: clearly

Deleted: wood anatomical

Deleted: s

SITE code	Mean value	CV	RBAR	n-EPS (0.85)
TASMANIA				
RCSrw	0.72	0.17	0.39	9.0
RCSewb	1.02	0.02	0.07	70.2
RCSlwb	0.58	0.05	0.18	25.6
RCSdb	0.45	0.08	0.17	27.3
MCKrw	0.75	0.13	0.40	8.5
MCKewb	1.19	0.01	0.20	22.5
MCKlwb	0.78	0.03	0.25	17.4
MCKdb	0.40	0.05	0.16	30.6
CMrw	0.71	0.10	0.31	12.9
CMewb	1.22	0.01	0.26	16.0
CMlwb	0.84	0.03	0.29	14.0
CMdb	0.36	0.05	0.19	23.5
MWWTRLrw	0.59	0.12	0.29	14.0
MWWTRLewb	1.23	0.01	0.14	34.9
MWWTRLlwb	0.82	0.03	0.15	31.1
MWWTRLdb	0.33	0.06	0.18	25.7
MRDrw	0.60	0.14	0.38	9.1
MRDewb	1.28	0.01	0.13	37.9
MRDlwb	0.88	0.03	0.21	21.2
MRDdb	0.40	0.07	0.21	21.3
MHPrw	0.36	0.13	0.39	8.9
MHPewb	1.06	0.02	0.28	14.7
MHPlwb	0.82	0.03	0.25	16.8
MHPdb	0.24	0.13	0.34	10.8
BUTrw	0.99	0.09	0.10	50.8
BUTewb	1.18	0.02	0.11	44.1
BUTlwb	0.63	0.06	0.11	47.0
BUTdb	0.58	0.07	0.10	52.9
NEW ZEALAND				
PKLrw	1.16	0.17	0.40	8.4
PKLewb	1.17	0.01	0.12	40.9
PKLlwb	0.83	0.02	0.07	73.7
PKLdb	0.34	0.05	0.10	52.6
HUPrw	1.39	0.15	0.27	15.4
HUPewb	1.03	0.01	0.04	126.7
HUPlwb	0.73	0.02	0.03	190.4
HUPdb	0.29	0.04	0.02	314.5
FLCrw	0.44	0.16	0.44	7.3
FLCewb	0.97	0.02	0.12	41.4
FLClwb	0.76	0.02	0.14	36.2
FLCdb	0.21	0.09	0.20	22.0
AHArw	0.49	0.09	0.30	13.0
AHAewb	0.07	0.02	0.13	38.8
AHALwb	0.04	0.05	0.16	29.6
AHADb	0.02	0.10	0.11	43.8
DPPrw	0.48	0.11	0.33	11.7
DPPewb	0.89	0.02	0.12	41.9
DPPlwb	0.69	0.02	0.08	65.9
DPPdb	0.21	0.07	0.07	73.9

671

672

673 Table A1: Mean RW, EWB, LWB and DB values for the raw chronologies. Coefficient of variation (CV) and mean inter-series
674 correlation (RBAR) are calculated from the 20-year spline detrended chronologies. n-EPS reflects the number of series needed to
675 attain an EPS value of 0.85 related to the RBAR value (Wilson and Elling 2004).

Deleted: s

TASMANIA

RCS - Celery Top

	RCSewb	RCSlwb	RCSdb
RCSrw	0.03	-0.64	0.67
RCSewb		0.22	0.27
RCSlwb			-0.82

MCK - Pencil Pine

	MCKewb	MCKlwb	MCKdb
MCKrw	-0.10	-0.41	0.45
MCKewb		0.57	-0.01
MCKlwb			-0.79

CM - Pencil Pine

	CMewb	CMIwb	CMdb
CMrw	0.01	-0.30	0.43
CMewb		0.68	-0.04
CMIwb			-0.71

MWWTRL - King Billy Pine

	MTewb	MTlwb	MTdb
MTrw	0.31	-0.40	0.62
MTewb		0.21	0.40
MTlwb			-0.76

MRD - King Billy Pine

	MRDewb	MRDlwb	MRDdb
MRDrw	0.18	-0.61	0.65
MRDewb		0.14	0.44
MRDlwb			-0.78

MHP - Huon Pine (high elevation)

	MHPewb	MHPlwb	MHPdb
MHPrw	0.64	-0.19	0.69
MHPewb		0.16	0.67
MHPlwb			-0.56

BUT - Huon Pine (low elevation)

	BUTewb	BUTlwb	BUTdb
BUTrw	-0.20	-0.49	0.31
BUTewb		0.21	0.35
BUTlwb			-0.72

NEW ZEALAND

PKL - Kauri

	PKLewb	PKLlwb	PKLdb
PKLrw	0.14	-0.37	0.54
PKLewb		0.44	0.42
PKLlwb			-0.55

HUP - Kauri

	HUPewb	HUPlwb	HUPdb
HUPrw	-0.02	-0.23	0.30
HUPewb		0.58	0.23
HUPlwb			-0.51

FLC - NZ Cedar

	FLCewb	FLClwb	FLCdb
FLCrw	0.40	-0.47	0.70
FLCewb		0.12	0.58
FLClwb			-0.66

AHA - Silver Pine

	AHAewb	AHALwb	AHAdb
AHArw	0.12	-0.29	0.38
AHAewb		0.48	0.32
AHALwb			-0.58

DPP - NZ Pink Pine

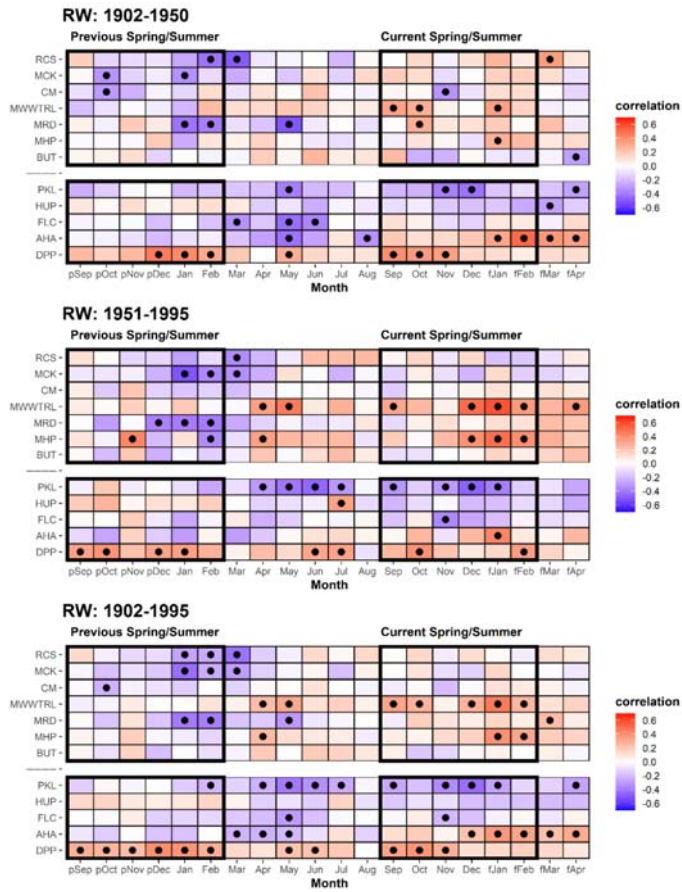
	DPPewb	DPPlwb	DPPdb
DPPrw	0.17	-0.25	0.51
DPPewb		0.60	0.60
DPPlwb			-0.20

677

678

679 Table A2: Correlation matrices for each site between the four detrended TR parameter chronologies (1798-1995). Grey shading
680 denotes a significant correlation (95%).

681

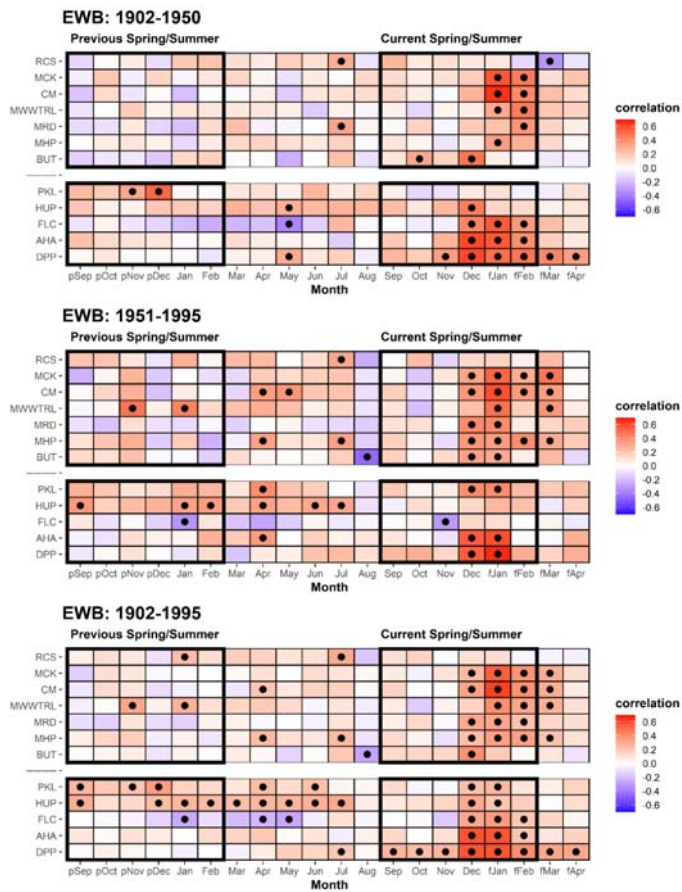


682

683

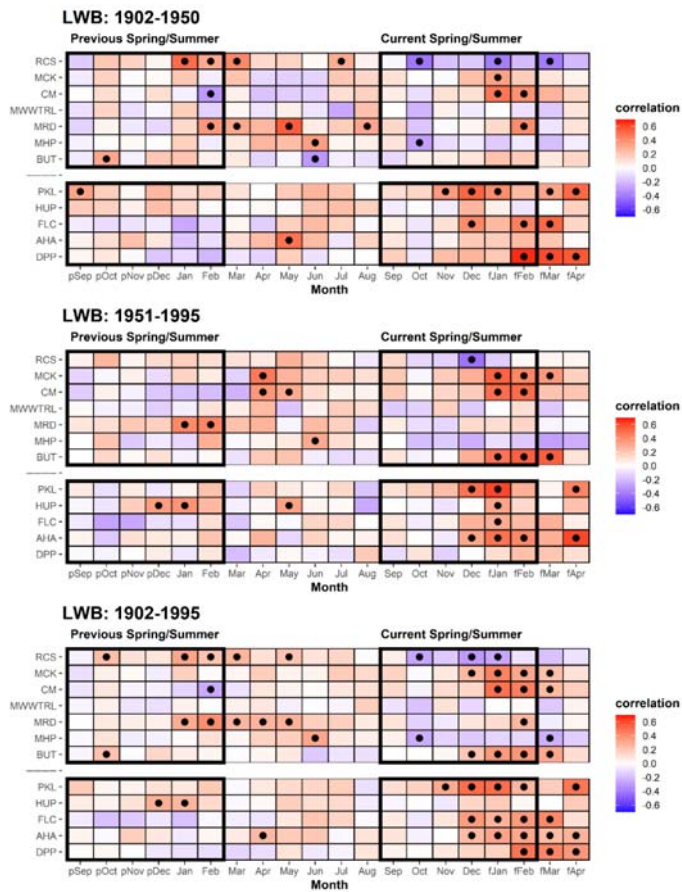
684 Table A3a: Correlation response function analysis for ring-width with CRU TS temperatures. Analysis was undertaken over the
685 1902-1950, 1951-1995 and 1902-1995 periods. Black dots denoted correlations significant at the 95% C.L.

686



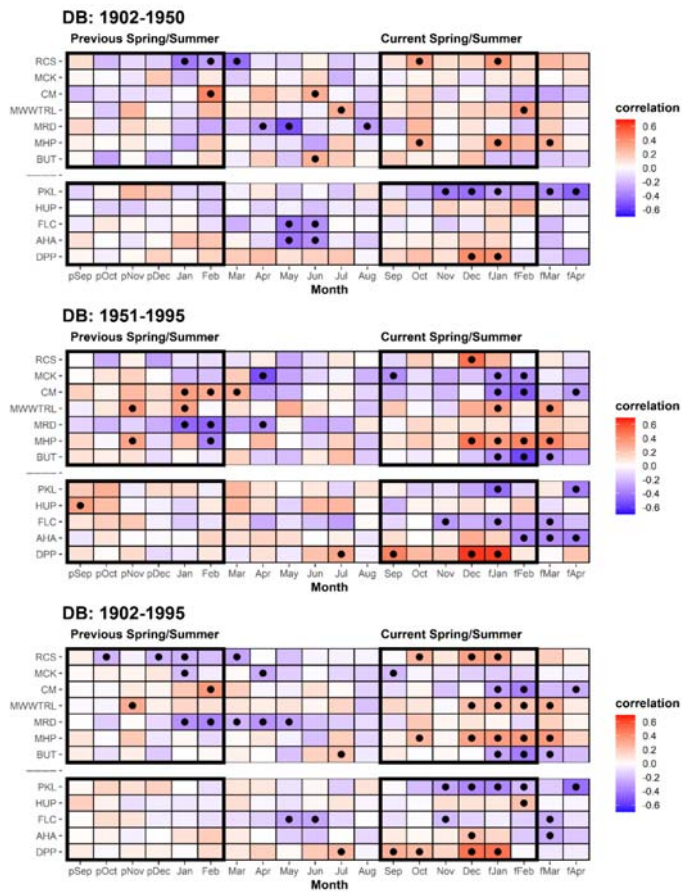
687

688 [Table A3b: As 3a but for EWB.](#)



689

690 [Table A3c: As 3a but for LWB.](#)

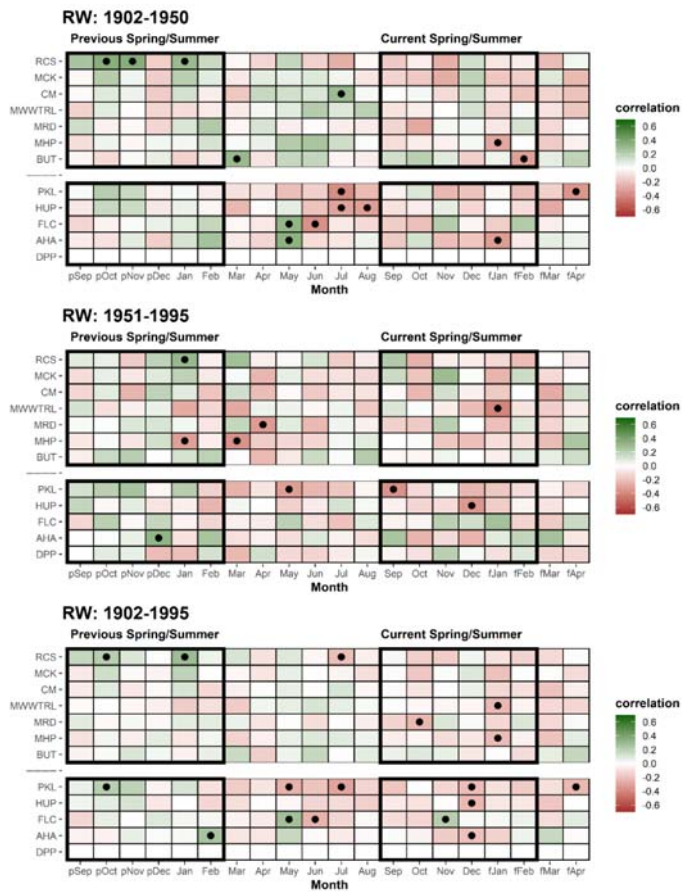


691

692 [Table A3d: As 3a but for DB.](#)

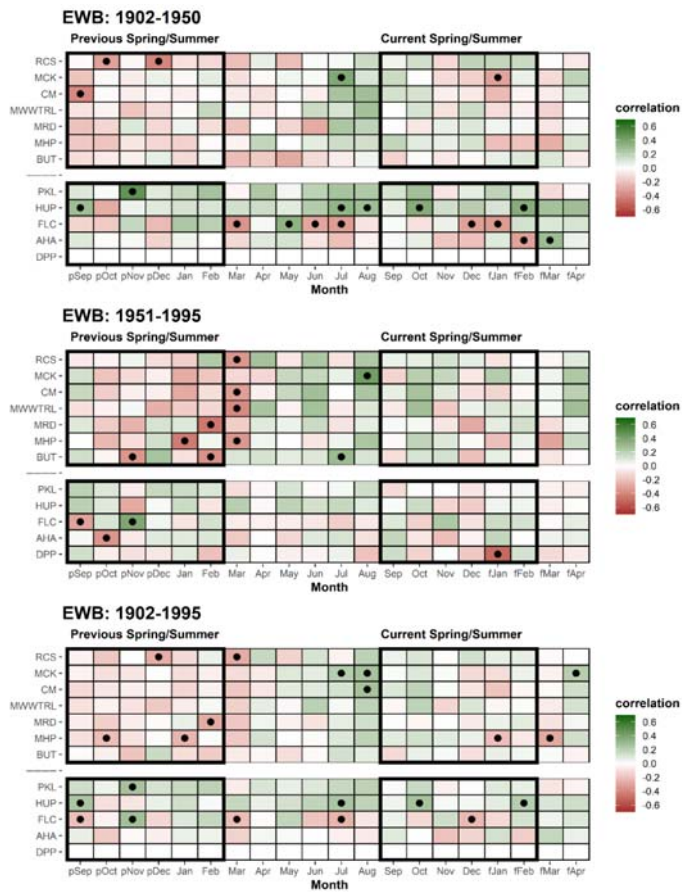
693

694



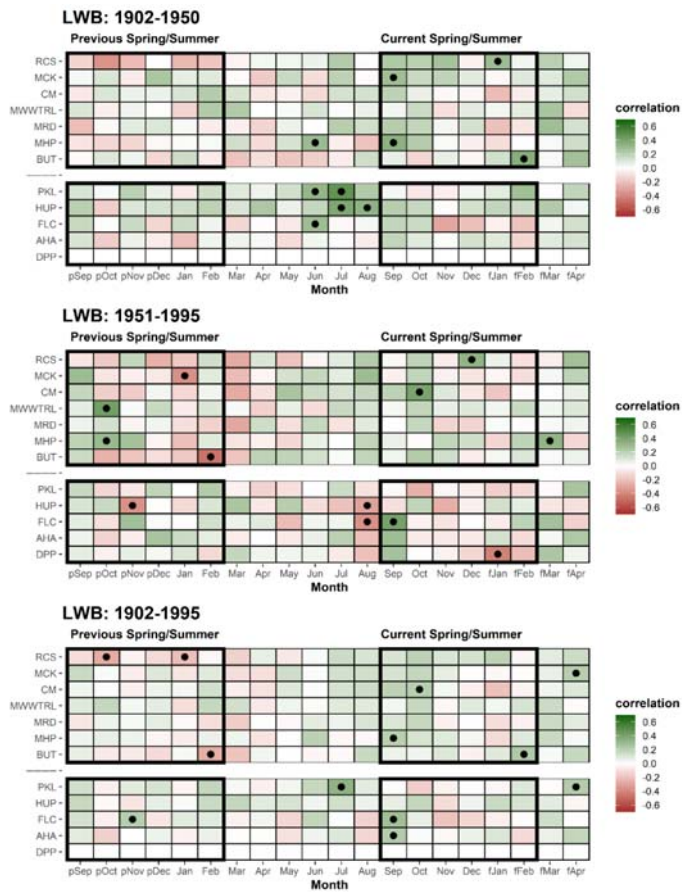
695

696 Table A4a: Correlation response function analysis for ring-width with CRU TS precipitation. Analysis was undertaken over the
 697 1902-1950, 1951-1995 and 1902-1995 periods. Black dots denoted correlations significant at the 95% C.L.



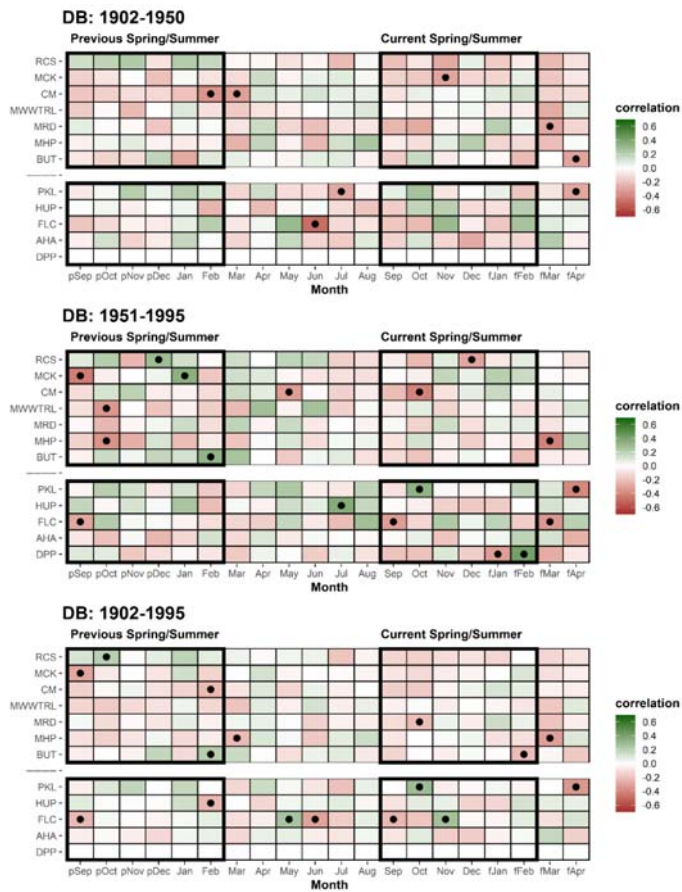
698

699 [Table A4b: As 4a but for EWB.](#)



700

701 [Table A4c: As 4a but for LWB.](#)

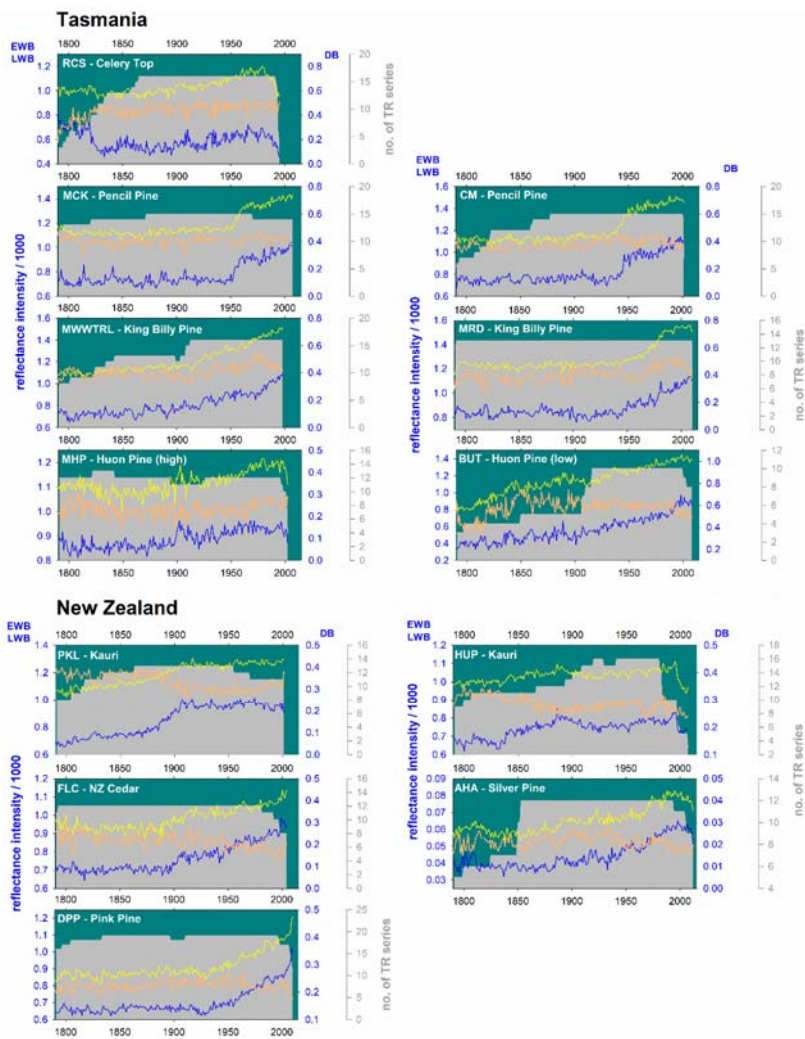


702

703 [Table A4d: As 4a but for DB.](#)

704

Formatted: Normal

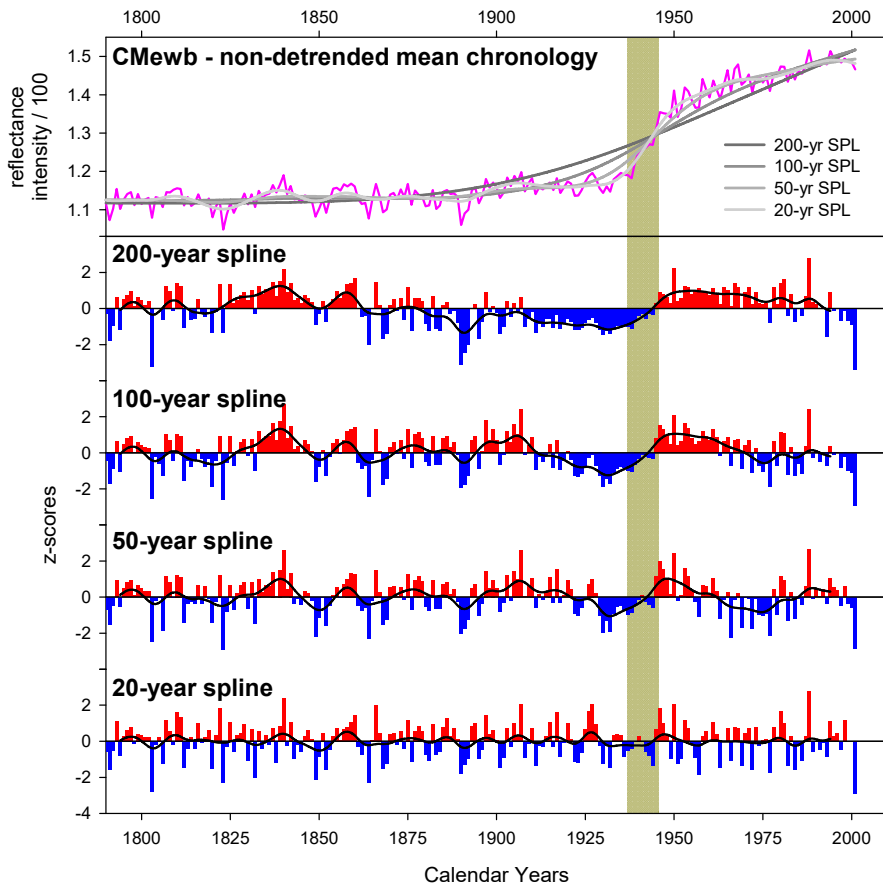


705

706 Figure A1: Plots of raw mean chronologies of EWB (yellow), LWB (blue), DB (orange) and TR series replication (grey shading).
 707 The left axis is for EWB and LWB, 1st right axis is DB, while 2nd right axis is series replication.

Deleted: bars
 Deleted: L

710



711

712

713 Figure A2: Upper panel: raw mean non-detrended EWB chronology for the CM Pencil Pine site. lower panel: represents
714 progressively more flexible spline detrending options. The vertical grey bar denotes the heartwood-gapwood transition period.

715

Deleted: V
Deleted: H
Deleted: S

719
720
721

722 **6 Data availability**

723 All raw data will be archived at the International Tree-Ring Databank on acceptance of the manuscript
724

725 **7 Author contribution**

726 RW: Project conception
727 RW, KA, PB, SB, GB, BB, EC, RD, AF, PK, JP: Sample collection and image acquisition
728 RW, KA, SB, MG: Data generation
729 All: Paper writing, final methodological design, comment and editing

730 **8 Competing interests**

731 The authors declare that they have no conflict of interest

732 **9 Acknowledgements**

733 RW was funded through the University of Melbourne Dyason Fellowship in 2014 to undertake preliminary measurement and
734 analyses for this study. Permission to obtain samples from the Tasmanian sites was provided by Parks and Wildlife
735 Tasmania through several different permits over multiple years. KA was supported by the Australian Research Council
736 grants DP1201040320 and LP12020811 to PB

Deleted: n

737 **10 References**

738 Allen, K.J., Cook, E.R., Francey, R.J. and Michael, K., 2001. The climatic response of *Phyllocladus aspleniifolius* (Labill.)
739 Hook. f in Tasmania. *Journal of Biogeography*, 28(3), pp.305-316.
740
741 Allen, K.J., Ogden, J., Buckley, B.M., Cook, E.R. and Baker, P.J., 2011. The potential to reconstruct broadscale climate
742 indices associated with southeast Australian droughts from *Athrotaxis* species, Tasmania. *Climate Dynamics*, 37(9-10),
743 pp.1799-1821.

745
746 Allen, K.J., Lee, G., Ling, F., Allie, S., Willis, M. and Baker, P.J., 2015a. Palaeohydrology in climatological context:
747 developing the case for use of remote predictors in Australian streamflow reconstructions. *Applied Geography*, 64, pp.132-
748 152.
749
750 Allen, K.J., Nichols, S.C., Evans, R., Cook, E.R., Allie, S., Carson, G., Ling, F. and Baker, P.J., 2015b. Preliminary
751 December–January inflow and streamflow reconstructions from tree rings for western Tasmania, southeastern Australia.
752 *Water Resources Research*, 51(7), pp.5487-5503.
753
754 Allen, K.J., Fenwick, P., Palmer, J.G., Nichols, S.C., Cook, E.R., Buckley, B.M. and Baker, P.J., 2017. A 1700-year
755 *Athrotaxis selaginoides* tree-ring width chronology from southeastern Australia. *Dendrochronologia*, 45, pp.90-100.
756
757 Allen, K.J., Cook, E.R., Evans, R., Francey, R., Buckley, B.M., Palmer, J.G., Peterson, M.J. and Baker, P.J., 2018. Lack of
758 cool, not warm, extremes distinguishes late 20th Century climate in 979-year Tasmanian summer temperature
759 reconstruction. *Environmental Research Letters*, 13(3), p.034041.
760
761 Alexander, M.R., Pearl, J.K., Bishop, D.A., Cook, E.R., Anchukaitis, K.J. and Pederson, N., 2019. The potential to
762 strengthen temperature reconstructions in ecoregions with limited tree line using a multispecies approach. *Quaternary*
763 *Research*, 92(2), pp.583-597.
764
765 Altman, J., 2020. Tree-ring-based disturbance reconstruction in interdisciplinary research: Current state and future
766 directions. *Dendrochronologia*, p.125733.
767
768 Arbellay, E., Jarvis, I., Chavardès, R.D., Daniels, L.D. and Stoffel, M., 2018. Tree-ring proxies of larch bud moth
769 defoliation: latewood width and blue intensity are more precise than tree-ring width. *Tree Physiology* 38(8), 1237-1245.
770
771 Babst, F., Poulter, B., Trouet, V., Tan, K., Neuwirth, B., Wilson, R., Carrer, M., Grabner, M., Tegel, W., Levanic, T. and
772 Panayotov, M., 2013. Site-and species-specific responses of forest growth to climate across the E uropean continent. *Global*
773 *Ecology and Biogeography*, 22(6), pp.706-717.
774
775 Babst, F., Wright, W.E., Szejner, P., Wells, L., Belmecheri, S., Monson, R.K., 2016. Blue intensity parameters derived from
776 *Ponderosa* pine tree rings characterize intra-annual density fluctuations and reveal seasonally divergent water limitations.
777 *Trees* 30(4), 1403-1415.
778

Deleted: p

780 Björklund, J.A., Gunnarson, B.E., Seftigen, K., Esper, J., Linderholm, H.W., 2014. Blue intensity and density from northern
781 Fennoscandian tree rings, exploring the potential to improve summer temperature reconstructions with earlywood
782 information. *Climate of the Past* 10(2), 877-885.
783

784 Björklund, J., Gunnarson, B.E., Seftigen, K., Zhang, P., Linderholm, H.W., 2015. Using adjusted blue intensity data to attain
785 high-quality summer temperature information: a case study from Central Scandinavia. *The Holocene* 25(3), 547-556.
786

787 Björklund, J., Seftigen, K., Schweingruber, F., Fonti, P., von Arx, G., Bryukhanova, M.V., Cuny, H.E., Carrer, M.,
788 Castagneri, D. and Frank, D.C., 2017. Cell size and wall dimensions drive distinct variability of earlywood and latewood
789 density in Northern Hemisphere conifers. *New Phytologist*, 216(3), pp.728-740.
790

791 Björklund, J., von Arx, G., Nievergelt, D., Wilson, R., Van den Bulcke, J., Günther, B., Loader, N.J., Rydval, M., Fonti, P.,
792 Scharnweber, T. and Andreu-Hayles, L. et al. 2019. Scientific merits and analytical challenges of tree-ring densitometry.
793 *Reviews of Geophysics*, 57(4), pp.1224-1264.
794

795 Björklund, J., Seftigen, K., Fonti, P., Nievergelt, D., von Arx, G., 2020. Dendroclimatic potential of dendroanatomy in
796 temperature-sensitive *Pinus sylvestris*. *Dendrochronologia* 60, 125673.
797

798 Blake, S.A., Palmer, J.G., Björklund, J., Harper, J.B. and Turney, C.S., 2020. Palaeoclimate potential of New Zealand
799 *Manoao colensoi* (silver pine) tree rings using Blue-Intensity (BI). *Dendrochronologia*, 60, p.125664.
800

801 Boswijk, G., Fowler, A.M., Palmer, J.G., Fenwick, P., Hogg, A., Lorrey, A. and Wunder, J., 2014. The late Holocene kauri
802 chronology: assessing the potential of a 4500-year record for palaeoclimate reconstruction. *Quaternary Science Reviews*, 90,
803 pp.128-142.
804

805 Bradley, R.S., 1999. *Paleoclimatology: reconstructing climates of the Quaternary*. Elsevier.
806

807 Briffa, K.R., Osborn, T.J., Schweingruber, F.H., Jones, P.D., Shiyatov, S.G. and Vaganov, E.A., 2002. Tree-ring width and
808 density data around the Northern Hemisphere: Part 1, local and regional climate signals. *The Holocene*, 12(6), pp.737-757.
809

810 Brookhouse, M. and Graham, R., 2016. Application of the minimum blue-intensity technique to a southern-hemisphere
811 conifer. *Tree-Ring Research*, 72(2), pp.103-107.
812

813 Buckley, B.M., Cook, E.R., Peterson, M.J. and Barbetti, M., 1997. A changing temperature response with elevation for
814 *Lagarostrobos franklinii* in Tasmania, Australia. In *Climatic Change at High Elevation Sites* (pp. 245-266). Springer,
815 Dordrecht.

816

817 [Buckley, B., Ogden, J., Palmer, J., Fowler, A. and Salinger, J., 2000. Dendroclimatic interpretation of tree-rings in *Agathis*](#)
818 [australis \(kauri\). 1. Climate correlation functions and master chronology. *Journal of the Royal Society of New Zealand*,](#)
819 [30\(3\), pp.263-276.](#)

820

821 Buckley, B.M., Hansen, K.G., Griffin, K.L., Schmiege, S., Oelkers, R., D'Arrigo, R.D., Stahle, D.K., Davi, N., Nguyen,
822 T.Q.T., Le, C.N. and Wilson, R.J., 2018. Blue intensity from a tropical conifer's annual rings for climate reconstruction: An
823 ecophysiological perspective. *Dendrochronologia*, 50, pp.10-22.

824

825 Büntgen, U., Krusic, P.J., Verstege, A., Sangüesa-Barreda, G., Wagner, S., Camarero, J.J., Ljungqvist, F.C., Zorita, E.,
826 Oppenheimer, C., Konter, O. and Tegel, W., 2017. New tree-ring evidence from the Pyrenees reveals Western Mediterranean
827 climate variability since medieval times. *Journal of Climate*, 30(14), pp.5295-5318.

828

829 Büntgen, U., Urban, O., Krusic, P.J., Rybníček, M., Kolář, T., Kyncl, T., Ač, A., Koňasová, E., Čáslavský, J., Esper, J. and
830 Wagner, S., 2021. Recent European drought extremes beyond Common Era background variability. *Nature Geoscience*,
831 14(4), pp.190-196.

832

833 Buras, A., 2017. A comment on the expressed population signal. *Dendrochronologia*, 44, pp.130-132.

834

835 Buras, A., Spyt, B., Janecka, K., Kaczka, R., 2018. Divergent growth of Norway spruce on Babia Góra Mountain in the
836 western Carpathians. *Dendrochronologia* 50, 33-43.

837

838 Camarero, J.J., Rozas, V. and Olano, J.M., 2014. Minimum wood density of *Juniperus thurifera* is a robust proxy of spring
839 water availability in a continental Mediterranean climate. *Journal of Biogeography*, 41(6), pp.1105-1114.

840

841 Camarero, J.J., Fernández-Pérez, L., Kirilyanov, A.V., Shestakova, T.A., Knorre, A.A., Kukarskih, V.V. and Voltas, J.,
842 2017. Minimum wood density of conifers portrays changes in early season precipitation at dry and cold Eurasian regions.
843 *Trees*, 31(5), pp.1423-1437.

844

845 Campbell, R., McCarroll, D., Loader, N.J., Grudd, H., Robertson, I., Jalkanen, R., 2007. Blue intensity in *Pinus sylvestris*
846 tree-rings: developing a new palaeoclimate proxy. *The Holocene* 17(6), 821-828.

Deleted: b

848
849 Campbell, R., McCarroll, D., Robertson, I., Loader, N.J., Grudd, H., Gunnarson, B., 2011. Blue intensity in *Pinus sylvestris*
850 tree rings: a manual for a new palaeoclimate proxy. *Tree-Ring Research* 67(2), 127-135.
851
852 Cleaveland MK (1986) climatic response of densitometric properties in semiarid site tree rings. *Tree-Ring Bull* 46:13–29
853
854 Cook, E.R. and Peters, K., 1981. The smoothing spline: a new approach to standardizing forest interior tree-ring width series
855 for dendroclimatic studies.
856
857 Cook, E. R. The Decomposition of Tree-Ring Series for Environmental Studies. *Tree-Ring Bulletin* 47 (1987): 37–59.
858
859 Cook, E.R., Briffa, K.R. and Jones, P.D., 1994. Spatial regression methods in dendroclimatology: a review and comparison
860 of two techniques. *International Journal of Climatology*, 14(4), pp.379-402.
861
862 Cook, E.R., Palmer, J.G., Cook, B.I., Hogg, A. and D'Arrigo, R., 2002. A multi-millennial palaeoclimatic resource from
863 *Lagarostrobos colensoi* tree-rings at Oroko Swamp, New Zealand. *Global and Planetary Change*, 33(3-4), pp.209-220.
864
865 Cook, E.R., Buckley, B.M., Palmer, J.G., Fenwick, P., Peterson, M.J., Boswijk, G. and Fowler, A., 2006. Millennia-long
866 tree-ring records from Tasmania and New Zealand: A basis for modelling climate variability and forcing, past, present and
867 future. *Journal of Quaternary Science: Published for the Quaternary Research Association*, 21(7), pp.689-699.
868
869 Cook, E.R. and Pederson, N., 2011. Uncertainty, emergence, and statistics in dendrochronology. In *Dendroclimatology* (pp.
870 77-112). Springer, Dordrecht.
871
872 D'Arrigo, R.D., Buckley, B.M., Cook, E.R. and Wagner, W.S., 1996. Temperature-sensitive tree-ring width chronologies of
873 pink pine (*Halocarpus biformis*) from Stewart Island, New Zealand. *Palaeogeography, Palaeoclimatology, Palaeoecology*,
874 119(3-4), pp.293-300.
875
876 [Davi, N.K., Rao, M.P., Wilson, R., Andreu-Hayles, L., Oelkers, R., D'Arrigo, R., Nachin, B., Buckley, B., Pederson, N.,](#)
877 [Leland, C. and Suran, B., 2021. Accelerated Recent Warming and Temperature Variability over the Past Eight Centuries in](#)
878 [the Central Asian Altai from Blue Intensity in Tree Rings. *Geophysical Research Letters*, p.e2021GL092933.](#)
879
880 Dolgova, E., 2016. June–September temperature reconstruction in the Northern Caucasus based on blue intensity data.
881 *Dendrochronologia* 39, 17-23.

882
883 Drew, D.M., Allen, K., Downes, G.M., Evans, R., Battaglia, M. and Baker, P., 2013. Wood properties in a long-lived conifer
884 reveal strong climate signals where ring-width series do not. *Tree Physiology*, 33(1), pp.37-47.
885
886 Druckenbrod, D.L., Pederson, N., Rentch, J. and Cook, E.R., 2013. A comparison of times series approaches for
887 dendroecological reconstructions of past canopy disturbance events. *Forest ecology and management*, 302, pp.23-33.
888
889 Duncan, R.P., Fenwick, P., Palmer, J.G., McGlone, M.S. and Turney, C.S., 2010. Non-uniform interhemispheric temperature
890 trends over the past 550 years. *Climate Dynamics*, 35(7-8), pp.1429-1438.
891
892 Esper, J., Frank, D.C., Timonen, M., Zorita, E., Wilson, R.J., Luterbacher, J., Holzkämper, S., Fischer, N., Wagner, S.,
893 Nievergelt, D. and Verstege, A., 2012. Orbital forcing of tree-ring data. *Nature Climate Change*, 2(12), pp.862-866.
894
895 Evans R. 1994. Rapid measurement of the transverse dimensions of tracheids in radial wood sections from *Pinus radiata*.
896 *Holzforschung* 48: 168–172.
897
898 Fonti, P., Bryukhanova, M.V., Myglan, V.S., Kirdyanov, A.V., Naumova, O.V. and Vaganov, E.A., 2013. Temperature-
899 induced responses of xylem structure of *Larix sibirica* (Pinaceae) from the Russian Altay. *American journal of botany*,
900 100(7), pp.1332-1343.
901
902 [Fowler, A., Palmer, J., Salinger, J. and Ogden, J., 2000. Dendroclimatic interpretation of tree-rings in *Agathis australis*](#)
903 [\(*kauri*\): 2. Evidence of a significant relationship with ENSO. *Journal of the Royal Society of New Zealand*, 30\(3\), pp.277-](#)
904 [292.](#)
905
906 Fowler, A.M., Boswijk, G., Lorrey, A.M., Gergis, J., Pirie, M., McCloskey, S.P., Palmer, J.G. and Wunder, J., 2012. Multi-
907 centennial tree-ring record of ENSO-related activity in New Zealand. *Nature Climate Change*, 2(3), pp.172-176.
908
909 Fritts, H.C., Smith, D.G., Cardis, J.W. and Budelsky, C.A., 1965. Tree-ring characteristics along a vegetation gradient in
910 northern Arizona. *Ecology*, 46(4), pp.393-401.
911
912 Fritts, H.C. 1976. *Tree Rings and Climate*. London: Academic Press Ltd.
913

Deleted: p

915 Fuentes, M., Salo, R., Björklund, J., Seftigen, K., Zhang, P., Gunnarson, B., Aravena, J.C., Linderholm, H.W., 2018. A 970-
916 year-long summer temperature reconstruction from Rogén, west-central Sweden, based on blue intensity from tree rings. *The*
917 *Holocene* 28(2), 254-266.

918

919 Harley, G.L., Heeter, K.J., Maxwell, J.T., Rayback, S.A., Maxwell, R.S., Reinemann, T.E. and H Taylor, A., 2020. Towards
920 broad-scale temperature reconstructions for Eastern North America using blue light intensity from tree rings. *International*
921 *Journal of Climatology*.

922

923 Harris, I.P.D.J., Jones, P.D., Osborn, T.J. and Lister, D.H., 2014. Updated high-resolution grids of monthly climatic
924 observations—the CRU TS3. 10 Dataset. *International journal of climatology*, 34(3), pp.623-642.

925

926 Heeter, K.J., Harley, G.L., Maxwell, J.T., McGee, J.H. and Matheus, T.J., 2020. Late summer temperature variability for the
927 Southern Rocky Mountains (USA) since 1735 CE: applying blue light intensity to low-latitude *Picea engelmannii* Parry ex
928 Engelm. *Climatic Change*, 162(2), pp.965-988.

929

930 Helama, S., Arentoft, B.W., Collin-Haubensak, O., Hyslop, M.D., Brandstrup, C.K., Mäkelä, H.M., Tian, Q. Wilson, R.,
931 2013. Dendroclimatic signals deduced from riparian versus upland forest interior pines in North Karelia, Finland. *Ecological*
932 *Research* 28(6), 1019-1028.

933

934 Kaczka, R.J., Spyt, B., Janecka, K., Beil, I., Büntgen, U., Scharnweber, T., Nievergelt, D., Wilmking, M., 2018. Different
935 maximum latewood density and blue intensity measurements techniques reveal similar results. *Dendrochronologia* 49, 94-
936 101.

937

938 [Kaczka, R.J. and Wilson, R., 2021. I-BIND: International Blue Intensity Network Development Working Group.](#)
939 [Dendrochronologia, p.125859.](#)

940

941 Kienast, F., Schweingruber, F.H., Bräker, O.U. and Schär, E., 1987. Tree-ring studies on conifers along ecological gradients
942 and the potential of single-year analyses. *Canadian Journal of Forest Research*, 17(7), pp.683-696.

943

944 Ljungqvist, F.C., Thejll, P., Björklund, J., Gunnarson, B.E., Piermattei, A., Rydval, M., Seftigen, K., Støve, B. and Büntgen,
945 U., 2020. Assessing non-linearity in European temperature-sensitive tree-ring data. *Dendrochronologia*, 59, p.125652.

946

947 Loader, N.J., Santillo, P.M., Woodman-Ralph, J.P., Rolfe, J.E., Hall, M.A., Gagen, M., Robertson, I., Wilson, R., Froyd,
948 C.A. and McCarroll, D., 2008. Multiple stable isotopes from oak trees in southwestern Scotland and the potential for stable
949 isotope dendroclimatology in maritime climatic regions. *Chemical Geology*, 252(1-2), pp.62-71.
950
951 Loader, N.J., Young, G.H., McCarroll, D., Davies, D., Miles, D. and Bronk Ramsey, C., 2020. Summer precipitation for the
952 England and Wales region, 1201–2000 [CE](#), from stable oxygen isotopes in oak tree rings. *Journal of Quaternary Science*.
953
954 Lorimer, C.G. and Frelich, L.E., 1989. A methodology for estimating canopy disturbance frequency and intensity in dense
955 temperate forests. *Canadian Journal of Forest Research*, 19(5), pp.651-663.
956
957 McCarroll, D., Pettigrew, E., Luckman, A., Guibal, F. and Edouard, J.L., 2002. Blue reflectance provides a surrogate for
958 latewood density of high-latitude pine tree rings. *Arctic, Antarctic, and Alpine Research*, 34(4), pp.450-453.
959
960 McCarroll, D. and Loader, N.J., 2004. Stable isotopes in tree rings. *Quaternary Science Reviews*, 23(7-8), pp.771-801.
961
962 Neukom, R., Gergis, J., Karoly, D.J., Wanner, H., Curran, M., Elbert, J., González-Rouco, F., Linsley, B.K., Moy, A.D.,
963 Mundo, I. and Raible, C.C., 2014. Inter-hemispheric temperature variability over the past millennium. *Nature Climate*
964 *Change*, 4(5), pp.362-367.
965
966 O'Donnell, A.J., Allen, K.J., Evans, R.M., Cook, E.R., Trouet, V. and Baker, P.J., 2016. Wood density provides new
967 opportunities for reconstructing past temperature variability from southeastern Australian trees. *Global and Planetary*
968 *Change*, 141, pp.1-11.
969
970 Palmer, J.G. and Xiong, L., 2004. New Zealand climate over the last 500 years reconstructed from *Libocedrus bidwillii*
971 *Hook. f.* tree-ring chronologies. *The Holocene*, 14(2), pp.282-289.
972
973 Panyushkina, I.P., Hughes, M.K., Vaganov, E.A. and Munro, M.A., 2003. Summer temperature in northeastern Siberia since
974 1642 reconstructed from tracheid dimensions and cell numbers of *Larix cajanderi*. *Canadian Journal of Forest Research*,
975 33(10), pp.1905-1914.
976
977 Prendin, A.L., Petit, G., Carrer, M., Fonti, P., Björklund, J. and von Arx, G., 2017. New research perspectives from a novel
978 approach to quantify tracheid wall thickness. *Tree Physiology*, 37(7), pp.976-983.
979

Deleted: ce

Deleted: p

982 Reid, E. and Wilson, R., 2020. Delta Blue Intensity vs. Maximum Density: A Case Study using *Pinus uncinata* in the
983 Pyrenees. *Dendrochronologia*, p.125706.
984
985 Rohde R, Muller RA, Jacobsen R et al. (2013) A new estimate of the average earth surface land temperature spanning 1753
986 to 2011. *Geoinformatics & Geostatistics: An Overview 1*: 1. doi: 10.4172/2327-4581.1000101.
987
988 Rydval, M., Larsson, L.Å., McGlynn, L., Gunnarson, B.E., Loader, N.J., Young, G.H., Wilson, R., 2014. Blue intensity for
989 dendroclimatology: should we have the blues? Experiments from Scotland. *Dendrochronologia* 32(3), 191-204.
990
991 Rydval, M., Druckenbrod, D., Anchukaitis, K.J. and Wilson, R., 2016. Detection and removal of disturbance trends in tree-
992 ring series for dendroclimatology. *Canadian Journal of Forest Research*, 46(3), pp.387-401.
993
994 Rydval, M., Loader, N.J., Gunnarson, B.E., Druckenbrod, D.L., Linderholm, H.W., Moreton, S.G., Wood, C.V. and Wilson,
995 R., 2017. Reconstructing 800 years of summer temperatures in Scotland from tree rings. *Climate Dynamics*, 49(9-10),
996 pp.2951-2974.
997
998 Rydval, M., Druckenbrod, D.L., Svoboda, M., Trotsiuk, V., Janda, P., Mikoláš, M., Čada, V., Bače, R., Teodosiu, M.,
999 Wilson, R., 2018. Influence of sampling and disturbance history on climatic sensitivity of temperature-limited conifers. *The*
1000 *Holocene* 28(10), 1574-1587.
1001
1002 Seftigen, K., Fuentes, M., Ljungqvist, F.C. and Björklund, J., 2020. Using Blue Intensity from drought-sensitive *Pinus*
1003 *sylvestris* in Fennoscandia to improve reconstruction of past hydroclimate variability. *Climate Dynamics*, pp.1-16.
1004
1005 St. George, S., 2014. An overview of tree-ring width records across the Northern Hemisphere. *Quaternary Science Reviews*,
1006 95, pp.132-150.
1007
1008 Trotsiuk, V., Pederson, N., Druckenbrod, D.L., Orwig, D.A., Bishop, D.A., Barker-Plotkin, A., Fraver, S. and Martin-Benito,
1009 D., 2018. Testing the efficacy of tree-ring methods for detecting past disturbances. *Forest Ecology and Management*, 425,
1010 pp.59-67.
1011
1012 Visser, H. and Molenaar, J., 1988. Kalman filter analysis in dendroclimatology. *Biometrics*, pp.929-940.
1013
1014 von Arx, G., Crivellaro, A., Prendin, A.L., Čufar, K. and Carrer, M., 2016. Quantitative wood anatomy—practical
1015 guidelines. *Frontiers in plant science*, 7, p.781.

1016
1017 Wang, L., Payette, S. and Bégoin, Y., 2002. Relationships between anatomical and densitometric characteristics of black
1018 spruce and summer temperature at tree line in northern Quebec. *Canadian Journal of Forest Research*, 32(3), pp.477-486.
1019
1020 Wigley, T.M., Briffa, K.R. and Jones, P.D., 1984. On the average value of correlated time series, with applications in
1021 dendroclimatology and hydrometeorology. *Journal of Applied Meteorology and Climatology*, 23(2), pp.201-213.
1022
1023 Wiles, G.C., Charlton, J., Wilson, R.J., D'Arrigo, R.D., Buma, B., Krapek, J., Gaglioti, B.V., Wiesenberg, N., Oelkers, R.,
1024 2019. Yellow-cedar blue intensity tree-ring chronologies as records of climate in Juneau, Alaska, USA. *Canadian Journal of*
1025 *Forest Research* 49(12), 1483-1492.
1026
1027 Wilmking, M., van der Maaten-Theunissen, M., van der Maaten, E., Scharnweber, T., Buras, A., Biermann, C., Gurskaya,
1028 M., Hallinger, M., Lange, J., Shetti, R. and Smiljanic, M., 2020. Global assessment of relationships between climate and tree
1029 growth. *Global Change Biology*, 26(6), pp.3212-3220.
1030
1031 Wilson, R.J. and Hopfmueller, M., 2001. Dendrochronological investigations of Norway spruce along an elevational transect
1032 in the Bavarian Forest, Germany. *Dendrochronologia*, 19(1), pp.67-79.
1033
1034 Wilson, R.J. and Luckman, B.H., 2003. Dendroclimatic reconstruction of maximum summer temperatures from upper
1035 treeline sites in Interior British Columbia, Canada. *The Holocene*, 13(6), pp.851-861.
1036
1037 Wilson, R. and Elling, W., 2004. Temporal instability in tree-growth/climate response in the Lower Bavarian Forest region:
1038 implications for dendroclimatic reconstruction. *Trees*, 18(1), pp.19-28.
1039
1040 Wilson, R.J.S, Rao, R., Rydval, M., Wood, C., Larsson, L.-A., Luckman, B.H. 2014. Blue Intensity for Dendroclimatology:
1041 The BC Blues: A Case Study from British Columbia Canada. *The Holocene* 24 (11), 1428-1438.
1042
1043 Wilson, R., Wilson, D., Rydval, M., Crone, A., Büntgen, U., Clark, S., Ehmer, J., Forbes, E., Fuentes, M., Gunnarson, B.E.,
1044 Linderholm, H., Nicolussi, K., Wood, C., Mills, C. 2017a. Facilitating tree-ring dating of historic conifer timbers using Blue
1045 Intensity. *Journal of Archaeological Science* 78, 99-111.
1046
1047 Wilson, R., D'Arrigo, R., Andreu-Hayles, L., Oelkers, R., Wiles, G., Anchukaitis, K., Davi, N., 2017b. Experiments based on
1048 blue intensity for reconstructing North Pacific temperatures along the Gulf of Alaska. *Climate of the Past* 13(8), 1007-1022.
1049

1050 Wilson, R., Anchukaitis, K., Andreu-Hayles, L., Cook, E., D'Arrigo, R., Davi, N., Haberbauer, L., Krusic, P., Luckman, B.,
1051 Morimoto, D., Oelkers, R., 2019. Improved dendroclimatic calibration using blue intensity in the southern Yukon. *The*
1052 *Holocene* 29(11), 1817-1830.

1053

1054 Xiong, L., Okada, N., Fujiwara, T., Ohta, S. and Palmer, J.G., 1998. Chronology development and climate response analysis
1055 of different New Zealand pink pine (*Halocarpus biformis*) tree-ring parameters. *Canadian Journal of Forest Research*, 28(4),
1056 pp.566-573.

1057

1058 Yasue, K., Funada, R., Kobayashi, O. and Ohtani, J., 2000. The effects of tracheid dimensions on variations in maximum
1059 density of *Picea glehnii* and relationships to climatic factors. *Trees*, 14(4), pp.223-229.

1060

1061 Young, G.H., Loader, N.J., McCarroll, D., Bale, R.J., Demmler, J.C., Miles, D., Nayling, N.T., Rinne, K.T., Robertson, I.,
1062 Watts, C. and Whitney, M., 2015. Oxygen stable isotope ratios from British oak tree-rings provide a strong and consistent
1063 record of past changes in summer rainfall. *Climate Dynamics*, 45(11-12), pp.3609-3622.